Provided for non-commercial research and education use.
Not for reproduction, distribution or commercial use.

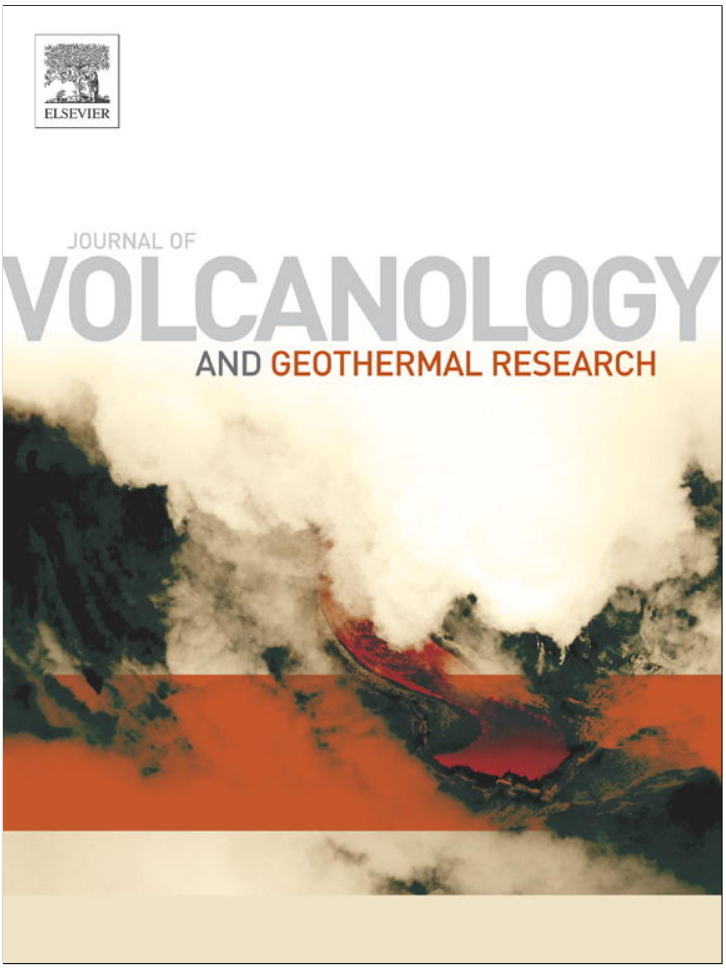

(This is a sample cover image for this issue. The actual cover is not yet available at this time.)

This article appeared in a journal published by Elsevier. The attached copy is furnished to the author for internal non-commercial research and education use, including for instruction at the authors institution and sharing with colleagues.

Other uses, including reproduction and distribution, or selling or licensing copies, or posting to personal, institutional or third party websites are prohibited.

In most cases authors are permitted to post their version of the article (e.g. in Word or Tex form) to their personal website or institutional repository. Authors requiring further information regarding Elsevier's archiving and manuscript policies are encouraged to visit:

http://www.elsevier.com/copyright

Author's personal copy

Journal of Volcanology and Geothermal Research 249 (2013) 77–94

Contents lists available at SciVerse ScienceDirect

Journal of Volcanology and Geothermal Research

journal homepage: www.elsevier.com/locate/jvolgeores

Structural control on geothermal circulation in the Cerro Tuzgle–Tocomar geothermal volcanic area (Puna plateau, Argentina)

Guido Giordano [a,*], Annamaria Pinton [a], Paola Cianfarra [a], Walter Baez [b], Agostina Chiodi [b], José Viramonte [b], Gianluca Norini [c], Gianluca Groppelli [c]

[a] Dipartimento di Scienze Geologiche, Università Roma Tre, Largo S. Leonardo Murialdo 1, 00146 Roma, Italy
[b] Instituto Geonorte, Facultad de Ciencias Naturales, Universidad Nacional de Salta, Salta, Argentina
[c] Istituto per la Dinamica dei Processi Ambientali — Sezione di Milano, Consiglio Nazionale delle Ricerche, Milano, Italy

ARTICLE INFO

Article history:
Received 10 June 2012
Accepted 12 September 2012
Available online 21 September 2012

Keywords:
Geothermal field
Structural lineaments
Secondary permeability
Remote sensing

ABSTRACT

The reconstruction of the stratigraphical–structural framework and the hydrogeology of geothermal areas is fundamental for understanding the relationships between cap rocks, reservoir and circulation of geothermal fluids and for planning the exploitation of the field. The Cerro Tuzgle–Tocomar geothermal volcanic area (Puna plateau, Central Andes, NW Argentina) has a high geothermal potential. It is crossed by the active NW–SE trans-Andean tectonic lineament known as the Calama–Olacapato–Toro (COT) fault system, which favours a high secondary permeability testified by the presence of numerous springs.

This study presents new stratigraphic and hydrogeological data on the geothermal field, together with the analysis from remote sensed image analysis of morphostructural evidences associated with the structural framework and active tectonics.

Our data suggest that the main geothermal reservoir is located within or below the Pre-Palaeozoic–Ordovician basement units, characterised by unevenly distributed secondary permeability. The reservoir is recharged by infiltration in the ridges above 4500 m a.s.l., where basement rocks are in outcrop. Below 4500 m a.s.l., the reservoir is covered by the low permeable Miocene–Quaternary units that allow a poor circulation of shallow groundwater. Geothermal fluids upwell in areas with more intense fracturing, especially where main regional structures, particularly NW–SE COT-parallel lineaments, intersect with secondary structures, such as at the Tocomar field. Away from the main tectonic features, such as at the Cerro Tuzgle field, the less developed network of faults and fractures allows only a moderate upwelling of geothermal fluids and a mixing between hot and shallow cold waters.

The integration of field-based and remote-sensing analyses at the Cerro Tuzgle–Tocomar area proved to be effective in approaching the prospection of remote geothermal fields, and in defining the conceptual model for geothermal circulation.

© 2012 Elsevier B.V. All rights reserved.

1. Introduction

The detailed study of the relationships between cap rocks, reservoir and circulation of geothermal fluids has been essential for identifying and developing the most productive geothermal fields in the world (Larderello and Latera in Italy, Barberi et al., 1984; Brogi, 2003; Taupo Volcanic Zone in New Zealand, Bibby et al., 1995; Wood, 1995; North America, Iceland and the Açores, Muffler and Duffield, 1995). More specifically, where fluid circulation is controlled by secondary permeability, the study of the fracture patterns plays a key role in understanding flow pathways in hydrothermal systems (e.g. Cox et al., 2001). The development of exploration and exploitation of geothermal energy in Argentina and other Andean regions is a very important goal, given the presence of a large heat anomaly associated with the magmatic arc, the renewability of the resource and the low environmental impact. Furthermore, the increasing connectivity across the Andes is increasing the potential end-users of such resource.

The area surrounding the Quaternary Cerro Tuzgle and Tocomar volcanic fields is located in the Puna plateau (NW Argentina, Allmendinger et al., 1997; Riller et al., 2001) and across the NW–SE Calama–Olacapato–Toro (COT) lineament (Ricci and Figueroa, 1971; Viramonte et al., 1984; Salfity, 1985; Matteini, 2002a,b), one of the major active tectonic lineaments in Central Andes (Fig. 1); it cuts through the entire Andean mountain belt from the Chilean forearc to the Argentinean foreland (Schurr et al., 1999). The area shows evidences of recent active tectonics (Petrinovic et al., 2006, 2010; Mazzuoli et al., 2008; Acocella et al., 2011) and several geothermal manifestations, including active and fossil hot-springs and travertine deposits. According to DeSilva and Gosnod (2007), magma intrusion rates in the Altiplano Puna during the last 10 Ma are an order of

* Corresponding author. Tel.: +39 06 57338004.
E-mail address: giordano@uniroma3.it (G. Giordano).

0377-0273/$ – see front matter © 2012 Elsevier B.V. All rights reserved.
http://dx.doi.org/10.1016/j.jvolgeores.2012.09.009

Author's personal copy

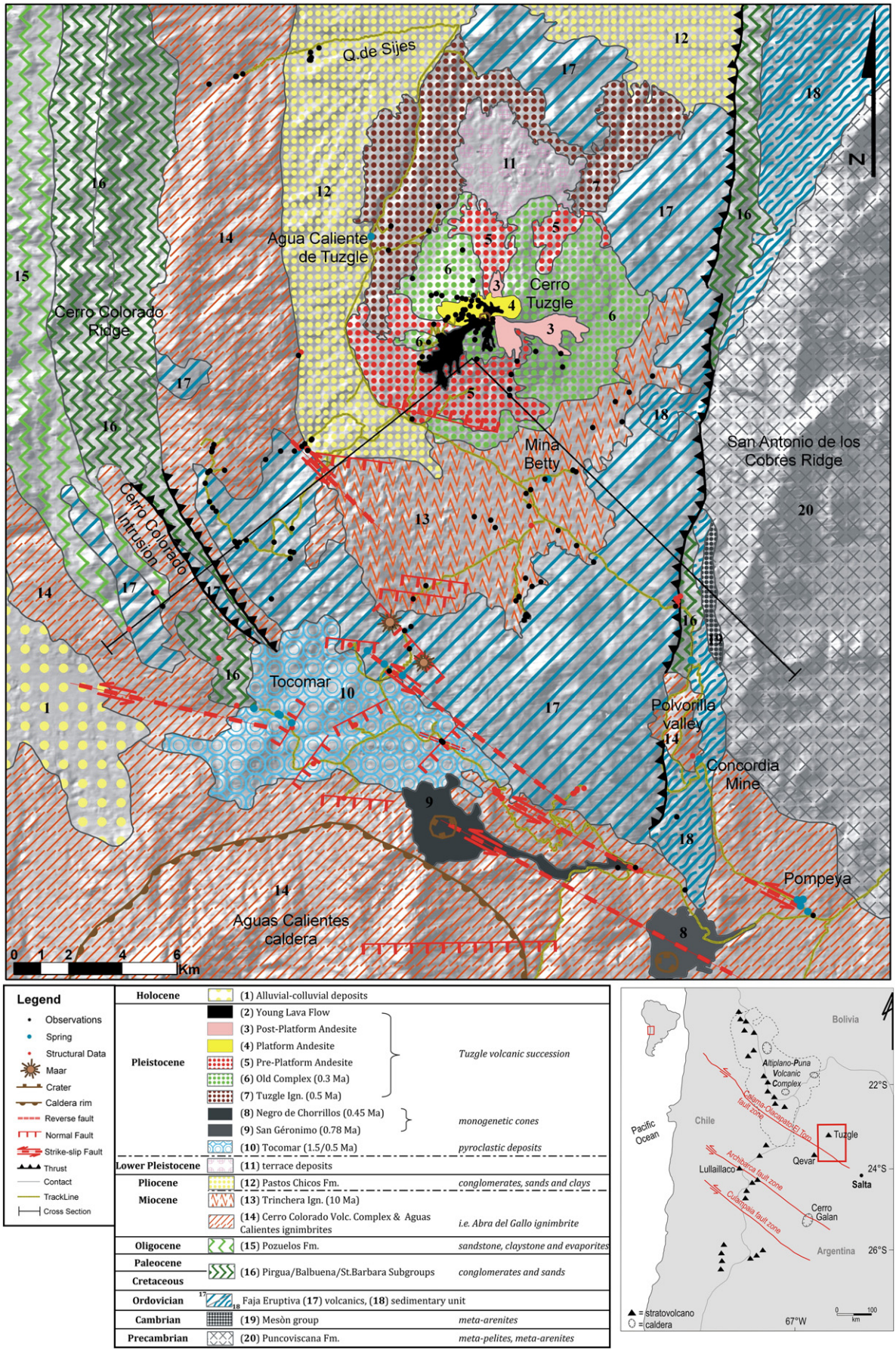

Fig. 1. Geological map of the study area. The inset box (bottom right) shows the main NW–SE left lateral faults that cross-cut the Central Andean region and the main volcanic centres. Modified with original field data from the 1:250,000 scale geological map of Blasco et al. (1996).

Author's personal copy

magnitude higher with respect to extrusion rates. All these evidences suggest the presence of a high geothermal potential in the Cerro Tuzgle–Tocomar area.

The Cerro Tuzgle and Tocomar geothermal fields are perfectly located for exploitation (Pesce, 2010), but presently not yet exploited. The local low enthalpy thermal springs of Pompeya, Tocomar and Aguas Caliente are along the main tourist roads connecting Argentina and Chile and could be used for thermal purposes favouring the development of a local sustainable tourism. A main electroduct connecting Chile and Argentina runs parallel to the COT aside the main Salta-Antofagasta road, securing an easy connection for electric power generation from middle to high enthalpy fluids. Furthermore, the many mining prospects existing in the area would also provide for future local customers along with the nearby towns of San Antonio de los Cobres and Olacapato.

The area was surveyed by numerous companies during the 1970s and 1980s [Aquater S.p.A., with Jujuy Mining Direction and Mining Secretary in 1980 (Aquater, 1980); Hidroproyectos SA-Setec SRL-Cepic SC in 1983–84 (Hidroproyectos et al., 1984); Jujuy Government, CREGEN and Universidad Nacional de Jujuy in 1987–88 (CREGEN, 1988)]. Preliminary studies (Coira and Kay, 1993; Coira, 1995; Sainato and Pomposiello, 1997) pointed out the existence of two reservoirs (a shallower and a deeper one) and of a young/active (<0.5 Ma) magma chamber associated with the Cerro Tuzgle volcano (Coira, 1995). The relationship between the structural framework and the circulation of geothermal fluids, however, was only reconstructed in its general features, since these studies were mainly based on geophysical and hydro-geochemical analyses. Similarly, rock formations that could form the seal and the reservoir were only inferred (Coira, 1995). The re-appraisal of the research aimed at the definition of the geothermal potential of the Cerro Tuzgle–Tocomar geothermal field is therefore important for the development of this rural part of Argentina.

This study presents the results of a multidisciplinary approach aimed at the understanding of the relationships between the circulation of geothermal fluids and the structural framework in the Cerro Tuzgle–Tocomar area. The new data set includes results of field stratigraphic and hydrogeological surveys of the geothermal field, the evaluation of the permeability of the main lithologies and the identification of morphostructural evidences associated with the structural framework and active tectonics from remote sensed image analysis.

2. Previous works on the Cerro Tuzgle and Tocomar geothermal fields

The Cerro Tuzgle–Tocomar geothermal field is associated with Miocene–Quaternary volcanic complexes, which overlie a polydeformed Pre-Cambrian–Ordovician basement and Cretaceous–Oligocene sedimentary successions (Fig. 1). Coira (1995) investigated the local magmatic source using geothermometers and geobarometers minerals from the 0.5 Ma Tuzgle ignimbrite unit (Fig. 1), estimating an eruption magma temperature of ~760 °C and a pressure of 2.5 to 3 kbar for the magma chamber; therefore the existence of a middle crustal magma chamber was assumed to be adequate for explaining the geothermal anomaly of the area. The magnetotelluric and gravimetric surveys supported the presence of the Cerro Tuzgle magma chamber, with its top below 8 km depth (Coira, 1995). According to later magnetotelluric and gravimetric surveys held by Sainato and Pomposiello (1997), the top of the magma chamber is located at 8 km depth; they described this chamber as a body partly filled with melted material and surrounded by free salt waters generated by chemical processes in the subducting plate. The chamber extends down to 22 km depth (Sainato and Pomposiello, 1997).

Both Aquater's (1980) and Coira's (1995) geoelectrical, magnetotelluric and gravimetric surveys, suggested the presence of a 100–600 m thick shallow reservoir at variable depths (50 to 300 m from the surface) associated with the 10 Ma Trinchera ignimbrite (Schwab, 1973), and capped by the sedimentary Miocene–Pliocene Pastos Chicos Fm. (Fig. 1). A slightly deeper reservoir was suggested at 2 km depth, with a thickness of some hundreds of metres, constituted by intensely fractured Ordovician rocks capped by the sedimentary Cretaceous Pirgua Subgroup (Coira, 1995; Sainato and Pomposiello, 1997). Sainato and Pomposiello (1997) also inferred the reservoir base at 3.1–3.6 km depth.

2.1. Geochemical data

The local thermal anomaly is represented by the presence of low-enthalpy hot springs, some exclusively with liquid emission (e.g. Tocomar and Mina Betty, Fig. 1) and others with both liquid and gaseous emissions (e.g. Pompeya and Aguas Calientes del Tuzgle) (Aguilera, 2008). According to CREGEN (1988), Tuzgle springs are of the alkaline-chloride type (Table 1), with conductivities of 1920 to 6710 μS/m and temperatures between 39 °C and 56 °C. Tocomar springs are also of the alkaline-chloride type, but they constitute a more homogenous group as conductivities range between 3300 and 3680 μS/m. Pompeya springs are of the chloride-alkaline type recording temperatures between 35 °C and 52 °C. Mina Betty is also of the alkaline-chloride type and its temperature is 21 °C.

Hydrothermal manifestations in the Tocomar geothermal field present incrustations, which are rich in SiO_2, SO_4 and CO_3 (Aquater, 1980) and have a magmatic signature (Ferretti, 1998). These manifestations sprout from local alluvial sediments and have produced travertine and

Table 1
Geochemical parameters determined for the geothermal springs of the Cerro Tuzgle–Tocomar area.

Thermal springs	Latitude	Longitude	Elevation	Temperature	Composition	Geothermometers
Baños de Pompeya	S 24° 14′ 802″	W 66° 21′ 755″	3854 m	56 °C[a,b]	Sodium chloride-bicarbonate[c]	Na–K-Ca[d] = 224.5 °C[b]; Na–K[d] = 212.5 °C[b]; Silica (Qz)[e] = 133.8 °C[b]
Mina Betty	S 24° 06′ 521″	W 66° 27′ 482″	4326 m	21 °C[a,b,f]	Alkaline chloride[f]	Na–K–Ca[d] = 186 °C[b]; Na–K[d] = 215 °C[b]; Silica (Qz)[e] = 156 °C[b]; K–Mg[g] = 82 °C[a]
Aguas Calientes del Tuzgle	S 24° 01′ 741″	W 66° 31′ 407″	4219 m	40–56 °C[a,b,f]	Alkaline chloride[f]	Na–K–Ca[d] = 217 °C[b]; Na–K[d] = 229 °C[b]; Silica (Qz)[e] = 156 °C[b]; K–Mg[g] = 125 °C[a]
Baños de Tocomar	S 24° 11′ 315″	W 66° 33′ 196″	4328 m	80 °C[h]	Sodium bicarbonate[c]	Na–K–Ca[d] = 227 °C[b]; Na–K[d] = 194 °C[b]; Silica (Qz)[e] = 151 °C[b]; K–Mg[g] = 115–160 °C[i]

[a] Sierra and Pedro (1988).
[b] Geotermia Andina (2008).
[c] Aguilera (2008).
[d] Fournier and Truesdell (1973).
[e] Fournier et al. (1974).
[f] Coira (1995).
[g] Giggenbach et al. (1983).
[h] Petrinovic et al. (2005).
[i] Ferretti and Alonso (1993).

Author's personal copy

silicified hydrothermal deposits (Pesce, 1999). The Pompeya area has two boreholes and numerous thermal springs that stem at the top of small travertine domes. The gaseous emissions of Pompeya indicate the presence of at least 30% of magmatic contribution supported by R/Ra values comprised between 2.49 and 2.55 (Hilton et al., 1993). N_2/Ar ratio is higher than the atmospheric one (N_2/Ar = 84); this indicates that part of N_2 comes from a non-atmospheric source. The gaseous emissions are enriched in alkenes, which suggests the presence of residual gases (Aguilera, 2008).

Geochemical parameters suggest that, to the west of Cerro Tuzgle, thermal waters are separated from cold ones by an impermeable barrier, while to the east, different zones can be identified in terms of mixing between hot and shallow cold waters (Coira, 1995). Moreover, important hydrochemical differences underline the existence of a separation between the Cerro Tuzgle geothermal field and the ones that develop along the COT lineament (Tocomar area) where mixtures between geothermal and surface waters were not detected (Coira, 1995).

The chemical characteristics of the liquid phase present in the Cerro Tuzgle–Tocomar geothermal systems indicate that the main water type produced is sodium-chloride waters or mature waters. These waters originated in deep reservoirs rich in Cl and Na, due to the dissolution of surrounding rocks. K–Mg and silica (chalcedony) geothermometers indicate reservoir temperatures of 134 and 143 °C respectively (Coira, 1995).

3. Stratigraphy and hydrogeological features

3.1. Stratigraphy

The Cerro Tuzgle–Tocomar area is wide and difficult to reach for a detailed field survey, therefore the stratigraphic reconstruction is based both on new field data and on generalisations based on satellite image analysis compared with existing geological maps for the area (Blasco et al., 1996). The reconstructed geology of the study area is shown in Fig. 1.

The hard-rock basement of the area is made by Pre-Cambrian–Eocambrian to Ordovician poly-deformed, low grade meta-sedimentary and meta-igneous rocks.

The oldest basement unit is the Pre-Cambrian Puncoviscana Fm. made of low grade, strongly deformed meta-pelites and meta-arenites (Turner, 1964; Aceñolaza and Aceñolaza, 2005). It crops out to the east of the study area and constitutes the N–S San Antonio ridge (Figs. 1 and 2a). Both the original lithology and the intense dominantly ductile deformation of the Puncoviscana Fm. make it the impermeable basement for the area.

Only in a narrow area along the west of San Antonio Ridge, the Puncoviscana Fm. is overlain by the Cambrian Méson Group (Fig. 1) made of more arenaceous lithologies.

The younger and much more widespread basement units in the area are the Ordovician metaintrusive, metavolcanic (known as Faja Eruptiva de la Puna, Mendez et al., 1973; Complejo Eruptivo Oire, Blasco et al., 1996) and metasedimentary rocks, which unconformably overlie the Puncoviscana Fm. (Coira, 1973; Viramonte et al., 2007) (Fig. 1). They are largely constituted by granites and volcanic rocks formed during the development of a magmatic arc in the early Palaeozoic, simultaneously with the emplacement of turbidites containing abundant volcaniclastic debris (Allmendinger et al., 1983). The Ordovician units crop out diffusely to the east of Cerro Tuzgle, along the ridge that overlooks on Polvorilla valley, and to the south along the COT lineament, being dominated in this area by the metaintrusive rocks (Fig. 1). The intrusive complex is intensely fractured and faulted. The jointing promotes a secondary permeability with spacing between 20 and 60 cm (Fig. 2b), often with quartz filling and variable openings, between 2 and 50 cm. In consideration of the large area of outcrop of the Ordovician rocks coinciding with the highest ridges, it can be assumed that they allow the recharge of the hydrogeological system.

Above the poly-deformed Pre-Cambrian and Palaeozoic basement rocks the oldest rocks preserved are Cretaceous–Oligocene syn-rift and post-rift sediments that were deposited along narrow grabens in rapid subsidence (Salfity and Monaldi, 2006). The Cretaceous Pirgua Subgroup (Reyes and Salfity, 1973) crops out to the east and west of Tuzgle where it unconformably overlies the basement (Fig. 2a). The main lithofacies are characterised by poorly sorted conglomerates and breccias, and fluvial–lacustrine sandstones, with a typical red-purple colour (Fig. 2c). The thickness in outcrop is up to 100 m although this is a minimum given the tectonics of the area (Fig. 2a). The coarse grain size and the poor cementation indicate that the Pirgua rocks represent a valuable permeable level. Evidence of permeability in the Pirgua breccias is found around the Concordia intrusion that caused extensive hydrothermal alteration of the clastic deposits (Fig. 2a). Elsewhere in the Andes, the Pirgua has also been identified as a geothermal reservoir, such as at Rosario de la Frontera geothermal area (Moreno Espelta et al., 1975; Seggiaro et al., 1997).

To the west of Cerro Colorado, the Pirgua Subgroup is overlain by the Santa Barbara Subgroup (Moreno, 1970) made of a stratified, dominantly pelitic continental succession. We have not observed directly the deposits of the intervening Balbuena Subgroup, although they have been mapped in the area (Blasco et al., 1996). Further to the west, Oligocene sedimentary rocks overlie the Santa Barbara Subgroup with a westward dip.

Miocene–Pliocene intrusive, volcanic and sedimentary rocks are present in the area accounting for the extensive magmatism of the Quechua tectonic phases (Reutter, 2001), 11–2 Ma, which formed the wide plateau of the Altiplano-Puna volcanic complex (APVC; DeSilva and Gosnod, 2007), folding and uplifting the Andean chain.

The Cerro Colorado ridge is extensively made of Miocene felsic domes and volcanics. To the east of Tuzgle, similar lavas intruded at the tectonic contact between the Ordovician basement and the Pirgua Subgroup along the Polvorilla valley (Fig. 2a), where the Concordia mine (Pb–Ag–Zn) was active till 1986 (Tonda et al., 2010).

Extensive ignimbrite sheets sourced between 11 and 10 Ma from the Aguas Caliente Caldera (Fig. 1). The Abra del Gallo dacitic ignimbrite crops out to the west of the COT. The ignimbrite is yellowish in colour, pumice rich and up to several tens of metres in thickness. Pumice is highly porphyritic and clasts are up to 7 cm. The ignimbrite was erupted at around 10.8 Ma (Petrinovic et al., 1999). The ignimbrite is extensively lithified by vapour-phase cement and characterised by m-spaced and generally closed cooling fractures; lithification reduces primary permeability and the wide fracture spacing accounts only for a low secondary permeability.

Similar in lithology to the Abra del Gallo ignimbrite, the dacite Trinchera ignimbrite crops out extensively around the Tuzgle volcano levelling the wide depression bounded by the N–S Cerro Colorado and S. Antonio ridges (Fig. 1). It is up to 30 m thick in outcrop, although the thickness may increase substantially towards the centre of the depression. Where the base is exposed, the ignimbrite unconformably covers the Ordovician basement. Trinchera Ig. was dated at 10 Ma (Schwab and Lippolt, 1976). It is a pinkish, ash-matrix supported partly welded lapilli tuff, which contains pumice clasts up to 10 cm. Pumice is highly porphyritic with quartz and biotite. Generally the accessory lithic content ranges 1–10% and is lapilli-sized (Fig. 2d). The ignimbrite is extensively lithified with diffuse vapour phase crystallisation of the matrix and shows well spaced vertical cooling fractures (5 to 6 m on average between fractures). Lithification of the matrix reduces the primary porosity and permeability of the ignimbrite (cf. Bear et al., 2009; Wright et al., 2011). Fractures generally are closed and do not show the occurrence of veins, suggesting also a low secondary permeability.

Towards the centre of the Tuzgle depression, the Trinchera Ig. is overlain by a sedimentary clastic succession of continental conglomerate, sand and siltstones which form the Upper Miocene–Pliocene Pastos Chicos Formation (Fig. 3). To the south, close to the source ridges, the Formation is dominated at the base by conglomerate lenses. The

Author's personal copy

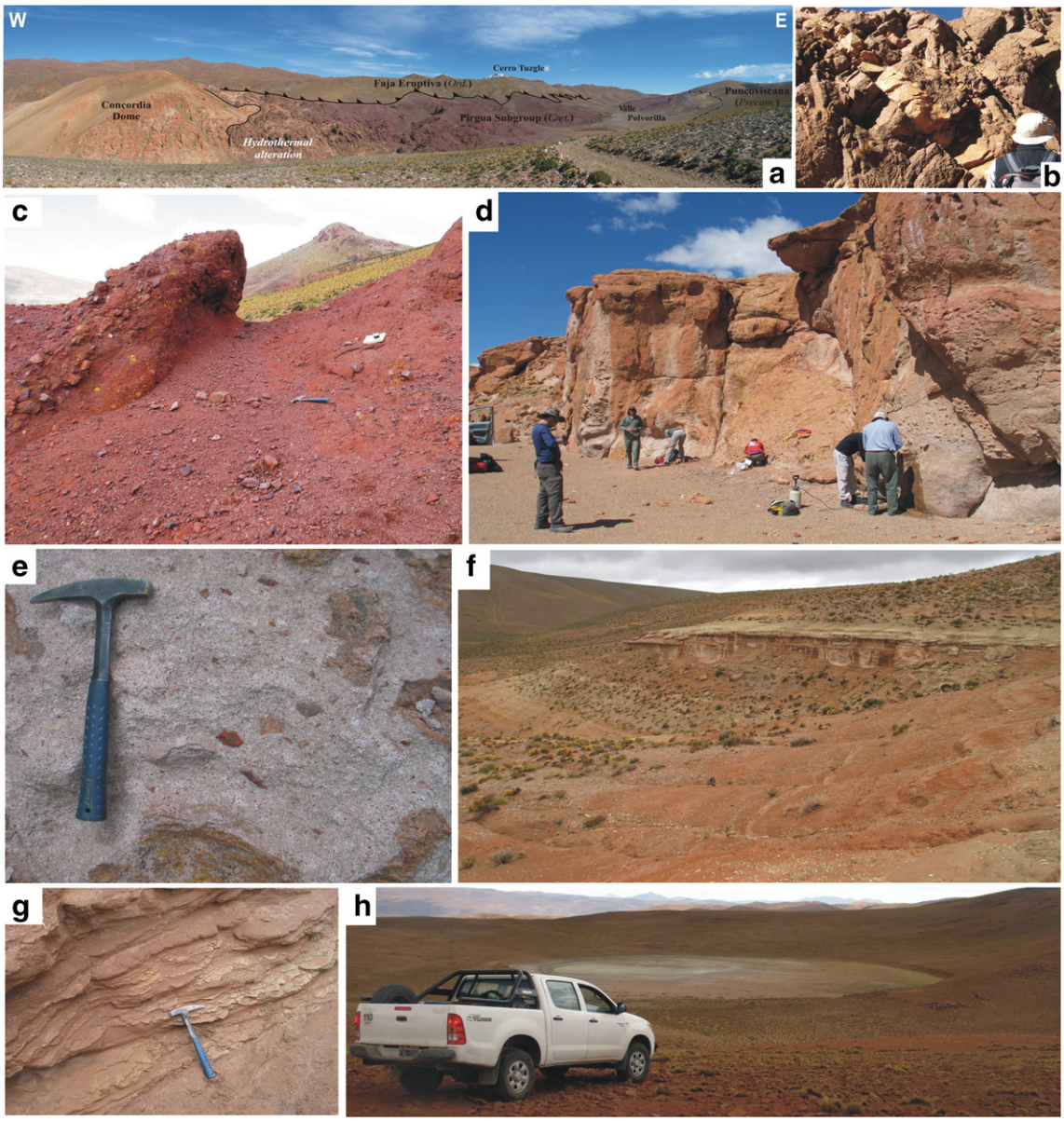

Fig. 2. (a) The main N–S thrust at Polvorilla valley with Ordovician Faja Eruptiva at hanging wall on the Cretaceous Pirgua Subgroup (dark red) which unconformably overlies the Pre-Cambrian Puncoviscana Formation; to the left (SW) the Pirgua Subgroup is intruded and hydrothermally altered by the Miocene Concordia rhyolitic dome; (b) Faja Eruptiva intrusive facies; note the narrow spaced fracturing that confers a good secondary permeability; (c) primary permeable conglomerate and breccias of the Pirgua Subgroup; (d) Trinchera ignimbrite, fractures are widely spaced and closed; (e) the ignimbrite is poorly permeable due to homogeneous fine grained and cemented lithology; (f) panoramic view of Pastos Chicos unit and (g) details on its fine ash layers; (h) one of the previously unidentified phreatic (or maar) craters which cut the Ordovician basement near the Tocomar geothermal area. (For interpretation of the references to colour in this figure legend, the reader is referred to the web version of this article.)

Formation thickens towards the north where it exceeds 70 m, and it is made of alternating sandstones and siltstones with interbedded ash tuffs (Figs. 3 and 2f,g), and travertine lenses. The succession shows a gradual upward coarsening and a concurrent decrease in the presence of volcanic material; this vertical variation could indicate a prograding fluvial system. The alternation of lithologies makes this unit highly variable in terms of permeability. However its restricted areal extent in the Cerro Tuzgle surroundings (Fig. 1) and very shallow position indicate that the Pastos Chicos Formation plays little to no role in the local hydrogeological system.

The Quaternary deposits of the area are associated with the scattered local volcanic and geothermal centres. The deposits associated with the San Géronimo, Negro de Chorrillos, Tocomar and Cerro Tuzgle centres (Fig. 1) have not been surveyed in detail, for their lithology, limited extent and very superficial stratigraphic position do not play any major role to the structure and circulation of the geothermal systems, although they are certainly permeable rocks for the zenithal recharge and indicate the presence of local conduits which may allow local preferential paths for geothermal fluids.

During the survey two localities have been recognised as previously unidentified phreatic pits or maars, located on the Ordovician ridge that bounds the COT near the Tocomar field (Figs. 1 and 2h). The two craters are aligned parallel to the COT, and have diameters of 300 m respectively and a bottom filled by clastic sediments made of basement derived m-sized blocks. Around the craters, only such type of lithic debris has been identified suggesting a most likely origin from phreatic explosions; however at some 4 km distance to the SE a thin succession of phreatomagmatic surge and fall deposits has been recognised, which might be related to those centres, in which case they would be classified as maars. These new discoveries indicate the presence at depth of pressurised fluids able to generate phreatic explosions in the hard-rock basement.

Author's personal copy

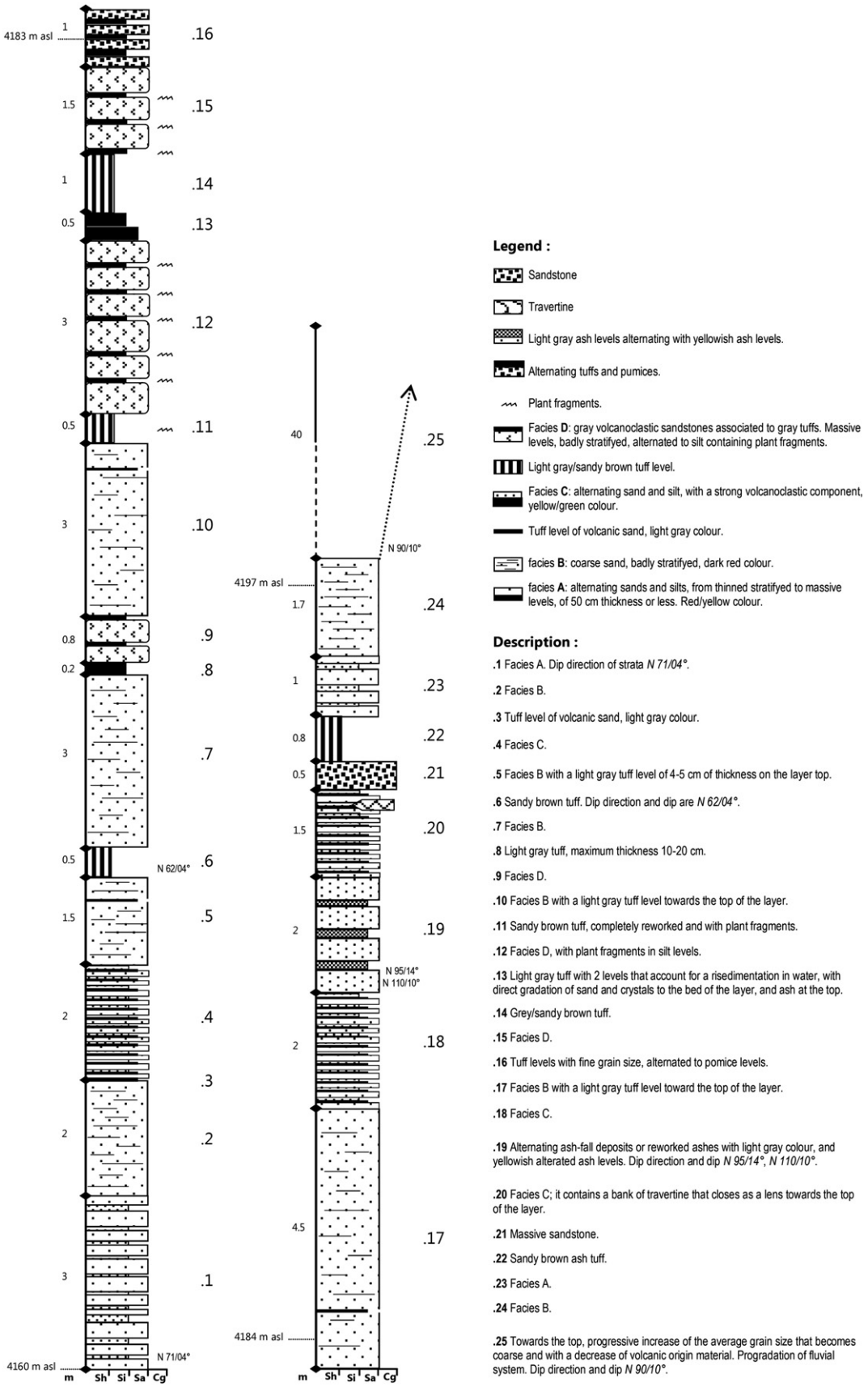

Fig. 3. Detailed stratigraphy of the Pastos Chicos unit section at the Quebrada de Sijes (location in Fig. 1), north of Tuzgle.

Author's personal copy

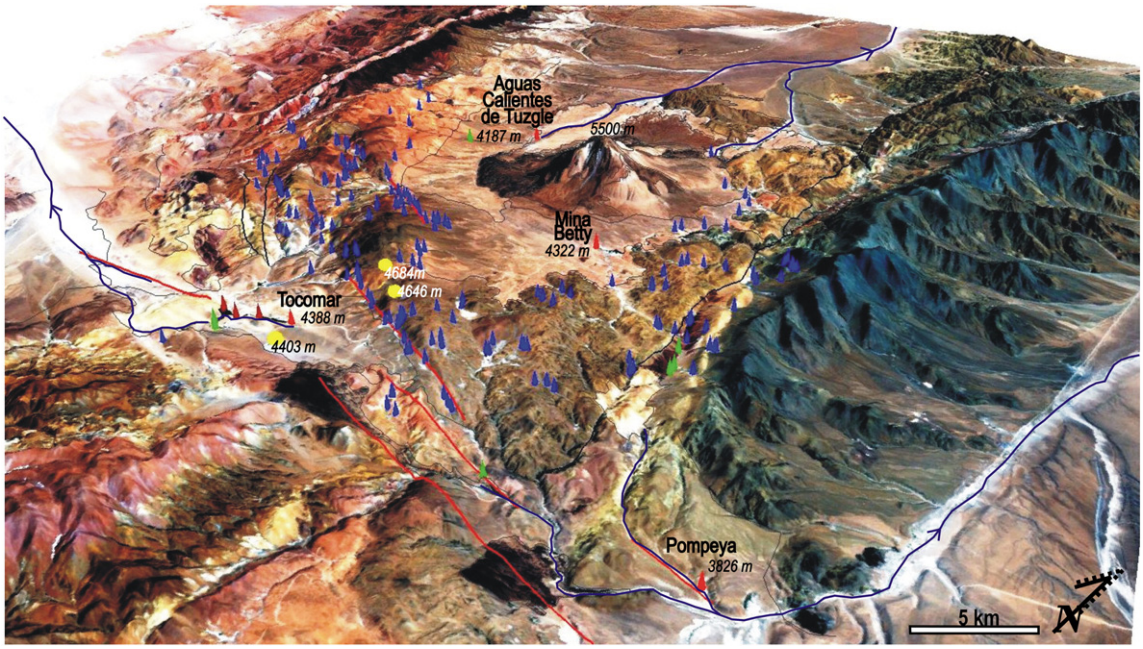

Fig. 4. Tridimensional view of the study area (from GoogleEarth). *Blue cones*: seasonal cold springs; *green cones*: permanent cold springs; *red cones*: thermal springs; *yellow circles*: maars; *red lines*: faults; *black lines*: thrusts; *grey lines*: lithologic contact as in Fig. 1. Permanent rivers are also indicated (*blue lines*) which flow towards three different endorheic depressions. Elevations of the main features are indicated. (For interpretation of the references to colour in this figure legend, the reader is referred to the web version of this article.)

3.2. Hydrogeological data

The area has an arid climate, characterised by very low precipitation, <100 mm/yr (Sobel et al., 2003). It is part of the larger Puna plateau intermontane hydrologically closed system, where surface waters flow towards endorheic depressions that form *salares* for evaporation (Sobel et al., 2003; Garcia-Castellanos, 2006). Two principal watersheds occur in the area: the first is the saddle transversal to the COT at the Tocomar volcanic field, where waters flow either to the NW or to the SE towards San Antonio de los Cobres (Fig. 4); the second watershed is the system of mountain ridges that encircles the Tuzgle depression and drains waters towards the N (Fig. 4).

Several permanent and seasonal springs have been surveyed at the time of the investigation (austral spring 2010), as well as other localities where groundwater surfaces along river channels feeding permanent flows (Fig. 4; Appendix 1). All groundwater emergences in the area have been surveyed and classified in terms of elevation and rock formation from which they issue (Fig. 5; Appendix 1). Based on the areal and elevation distributions of rock formations, springs (Table 2; Fig. 5) and locations with respect to the main watersheds we can define the following main hydrogeological characteristics:

(1) the main permanent springs which feed permanent rivers are located at the bottom of incised valleys at elevations comprised between 4400 and 4200 m a.s.l. and issue from both the basement and the Tertiary cover rocks. Permanent springs also occur at lower elevations;

Table 2
Statistics of outcropping rock-formations based on geology, draped on a 30 m-resolution DEM.

ID	Unit	Area (km^2)	Elevation					
			Min	Max	Range	Mean	Median	St. dev
1	Alluvial–colluvial deposits	29.95	4071	4490	419	4173.61	4157	71.09
2	Young lava flow	2.63	4466	5466	1000	4863.66	4781	299.86
3	Post-platform andesite	3.29	4397	5455	1058	4837.00	4803	256.99
4	Platform andesite	2.20	4702	5454	752	5112.21	5123	156.27
5	Pre-platform andesite	23.93	4159	5124	965	4474.88	4460	129.53
6	Old complex	36.18	4237	5486	1249	4486.84	4426	201.90
7	Tuzgle Ig.	38.12	3989	4460	4460	4176.21	4184	126.52
8	Negro de Chorrillos	5.88	3854	4391	537	4029.53	3997	130.97
9	San Géronimo	8.53	3980	4930	950	4512.71	4527	211.73
10	Tocomar deposits	41.41	4248	4639	391	4439.61	4434	66.31
11	Terrace deposits	12.66	4089	4373	284	4218.51	4217	43.27
12	Pastos Chicos Fm.	89.94	3935	4675	740	4202.69	4181	172.31
13	Trinchera Ig.	61.82	4186	4950	764	4435.78	4385	150.62
14	Cerro Colorado volc. complex and Aguas Cal. Ig.	334.61	3771	5442	1671	4478.84	4485	319.53
15	Pozuelos Fm.	55.98	4182	4719	537	4374.47	4363	96.79
16	Pirgua/Balbuena/St. Barbara Subgroups	95.14	4009	5047	1038	4525.52	4546	209.46
17	Ordov. Faja Eruptiva	176.48	3953	5107	1154	4460.13	4456	215.90
18	Ordov. sedimentary units	51.33	3896	4492	4492	4169.25	4168	143.90
19	Méson group	2.33	4334	4562	228	4450.25	4449	54.76
20	Puncoviscana Fm.	158.70	3752	4984	1232	4227.11	4236	281.33

Legend: total area covered by each unit, minimum and maximum elevations, range of elevations, arithmetic mean, median and standard deviation of elevations.

Author's personal copy

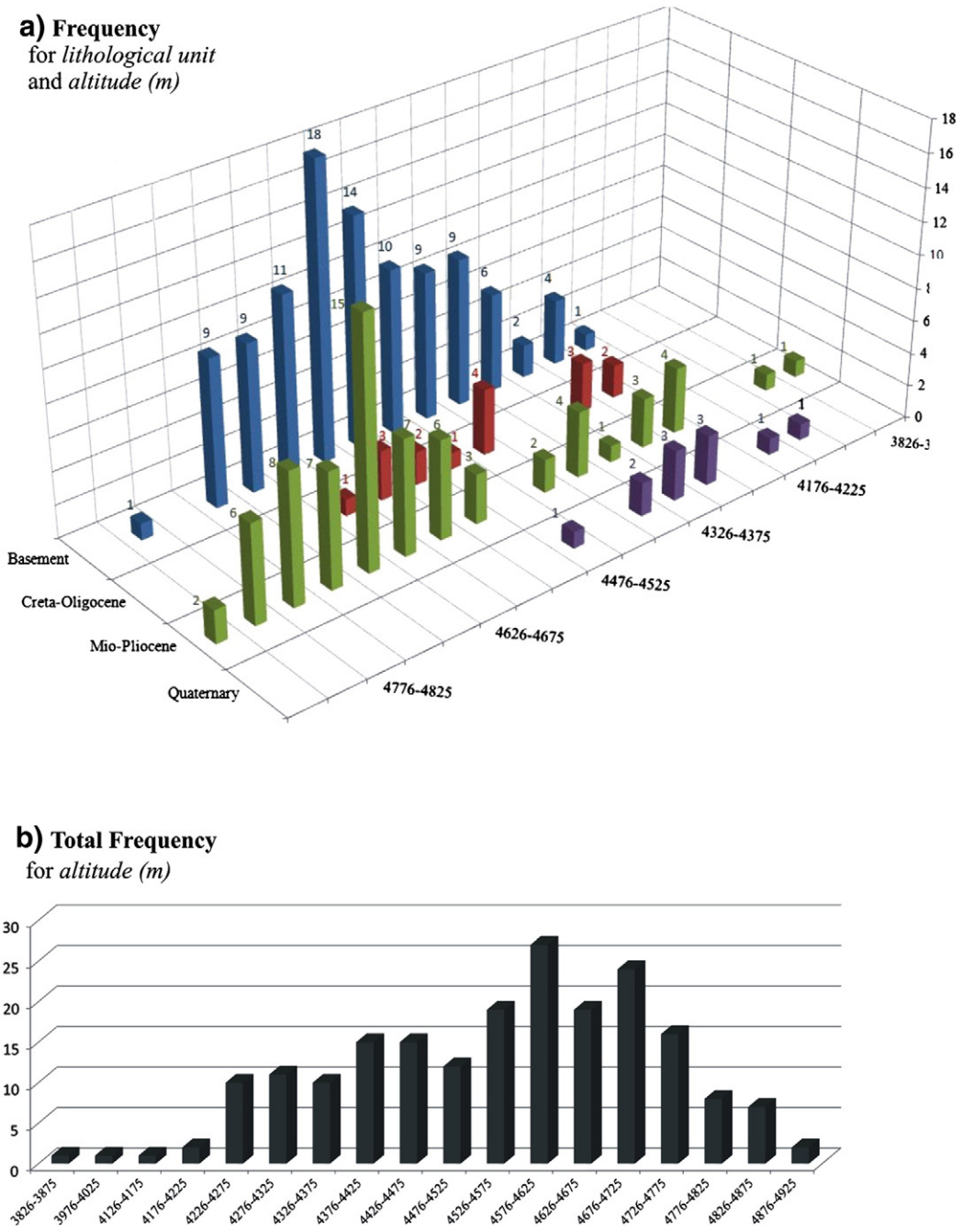

Fig. 5. (a) 3D histogram showing the number of springs (frequency) located within each lithological group and arranged for different elevation intervals; (b) histogram showing the total number of springs for different elevation intervals.

(2) most of the seasonal springs occur above 4500 m a.s.l. and are located in the Pre-Cambrian–Ordovician basement rocks or in the Miocene Cerro Colorado igneous rocks (Fig. 5), all characterised by secondary permeability; these formations also have the largest outcrop areas and have mean elevations higher than 4400 m a.s.l. (Table 2);
(3) consequently, the main recharge areas are the ridges that bound the Tuzgle depression above 4400 m;
(4) all main rivers in the area have their permanent feeding springs directly from or close to the main geothermal springs of the area (Fig. 4) (e.g. Tocomar, Aguas Caliente, Mina Betty, Pompeya thermal springs). Therefore the buoyancy of hot waters from the hydrothermal system plays a fundamental role in the shallow dynamics of the local hydrogeology;
(5) the number of springs issuing from the Tertiary volcanic and sedimentary cover is little in spite of the lower average elevation (4385 m for the Trinchera Ig. and 4181 m for the Pastos Chicos Fm.) and relatively large areal extent (Fig. 5; Table 2); these features can be interpreted in two opposite ways, i.e. these rocks are either impermeable allowing only the runoff of water, or alternatively highly permeable allowing fast infiltration and low hydraulic gradients. The first option is favoured by the presence of a significant erosional drainage network that cuts through these rocks. Furthermore, the lithologies observed for these rocks are poorly permeable, suggesting that the Tertiary rocks play the role of a poorly permeable cover likely hosting a poorly productive shallow aquifer fed by the basement rocks both laterally and from below, where hot waters upwell along main fracture zones.

Author's personal copy

3.3. Reinterpretation of geoelectric data

The reinterpretation of the Vertical Electric Soundings (VES) performed by HIDROPROYECTOS S.A. (unpublished data, courtesy of Dr. Giorgio Stangalino, Senior geophysicist at AREA GEOFISICA ENG. S.A. — Buenos Aires, Argentina) shows that the Cerro Tuzgle field is characterised by two main geoelectrical units (Fig. 6a). The low resistivity cover, on average 200–600 m thick with values > 8–10 Ωm overlies a resistive basement characterised by values > 500 Ωm (800 Ωm on average). The low resistivity cover thickens in correspondence to abrupt downthrows of the basement, interpreted as faults. Locally, close to the Aguas Calientes thermal spring, lower values of the resistivity, < 5 Ωm, are observed, both in the basement and in the cover. The basement shows 1.2 Ωm low values confined in a vertical geometry, whereas in

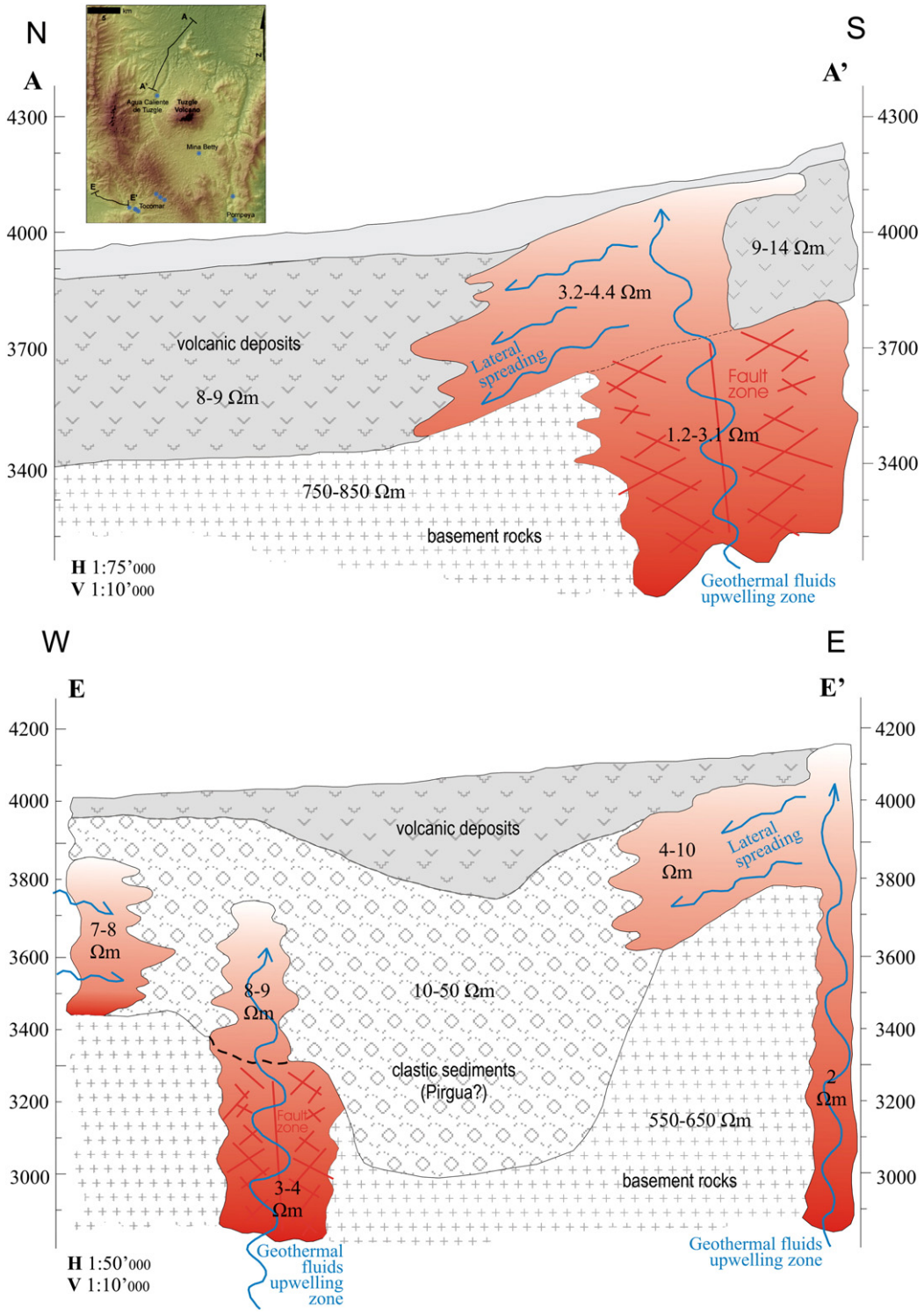

Fig. 6. Reinterpreted geoelectric profiles for the Cerro Tuzgle (a) and Tocomar (b) geothermal fields.
The first order geometries of electro-magnetic units and resistivity value ranges are unpublished data, courtesy of Dr. Giorgio Stangalino, Senior geophysicist at AREA GEOFISICA ENG. S.A. — Buenos Aires, Argentina.

Author's personal copy

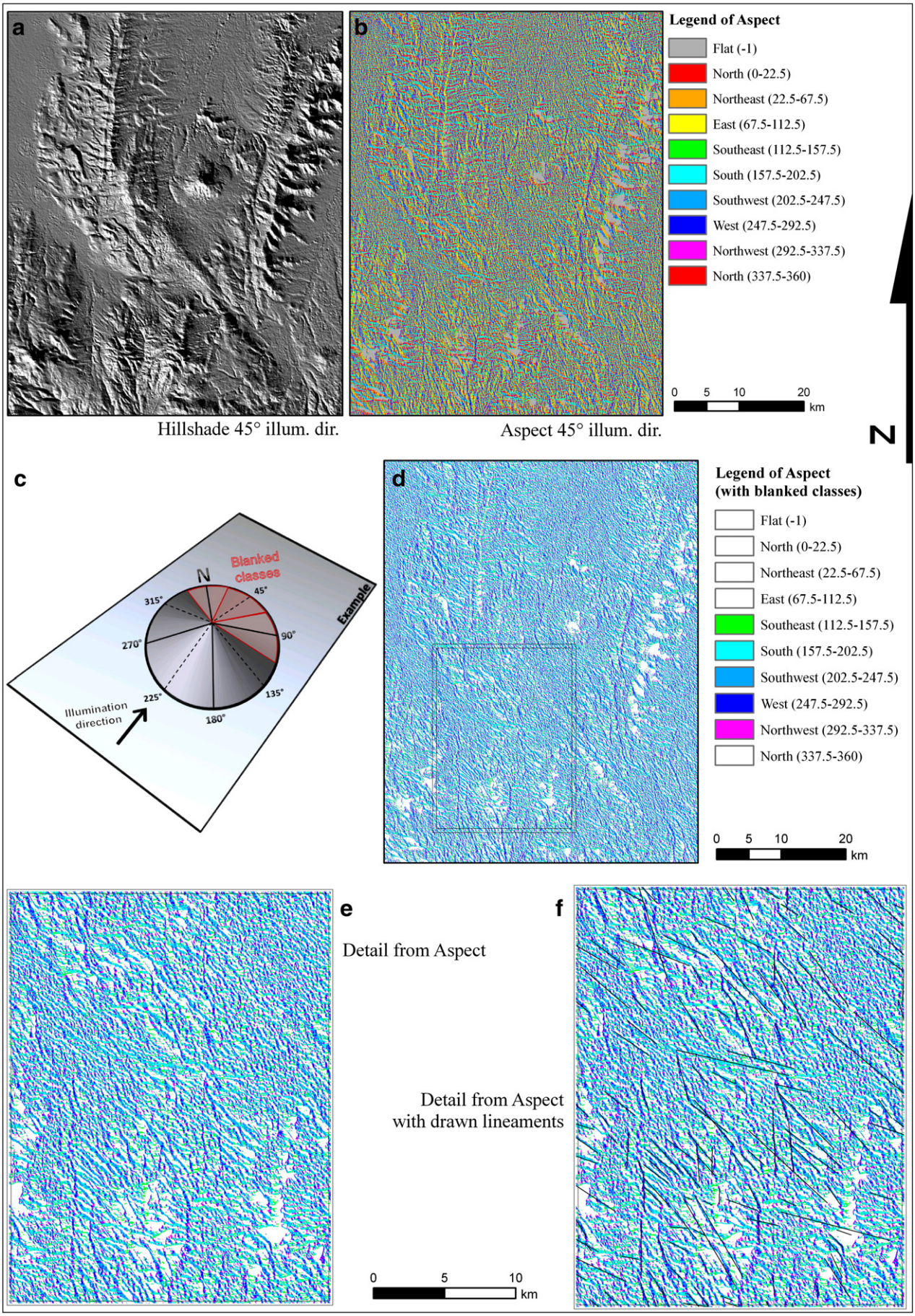

Author's personal copy

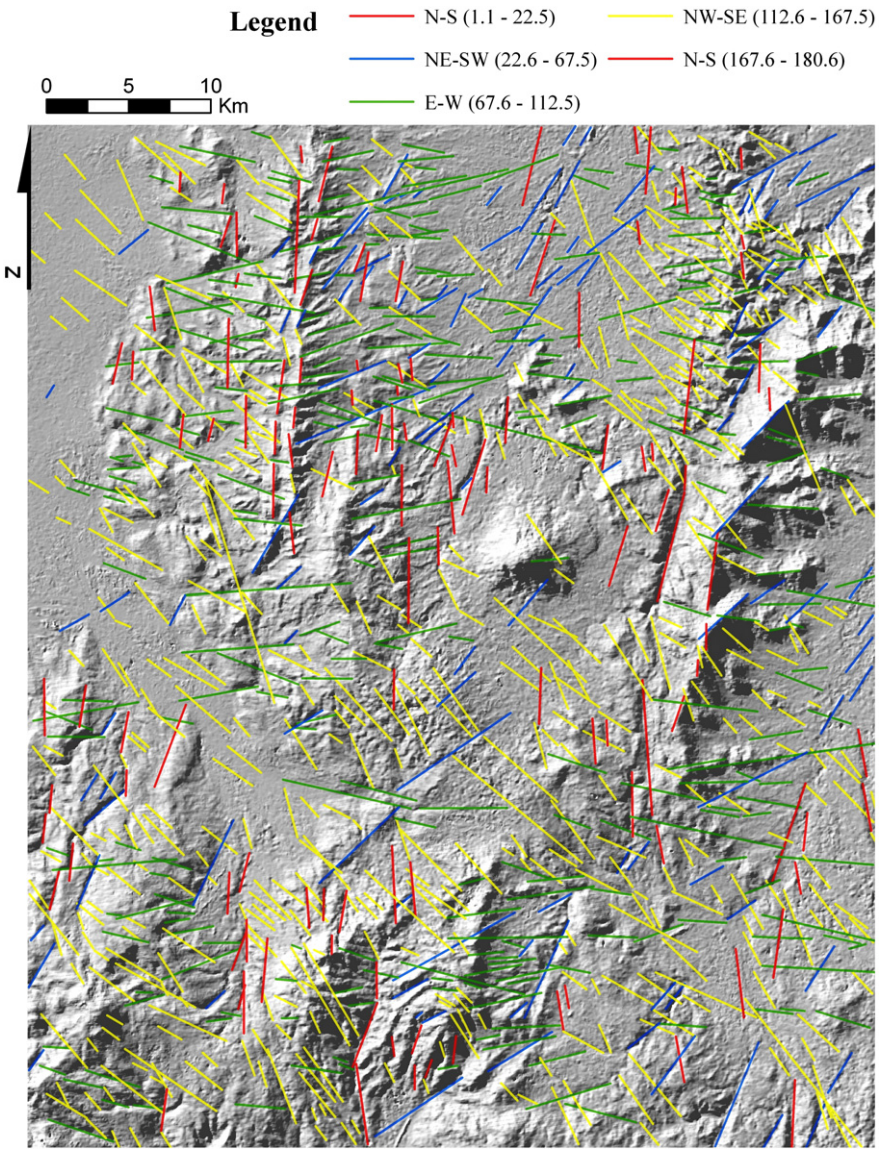

Fig. 8. Hillshade of the area with all the lineaments manually detected, subdivided in orientation classes (legend).

the cover, resistivity values are higher (3.2–4.4 Ωm) and increase up to 9 Ωm away from the main anomaly area pertaining (= permeating) to the entire cover geometry. Based on the surface geology, the low resistivity cover can be associated with the Trinchera Ig. and Pastos Chicos Fm., which unconformably overlie the resistive Ordovician basement. The upwelling of hydrothermal fluids can only be associated with areas where the resistivity drops below 5 Ωm. The observed geometries suggest that fluids upwell through the basement along vertical fractures, and then spread laterally into the shallow aquifer hosted by the poorly porous rocks which form the cover.

The Tocomar field shows a similar electrostratigraphy to the Cerro Tuzgle field (Fig. 6b). The low resistivity cover (10–50 Ωm) is 400–1000 m thick and overlies a resistive basement (>400 Ωm). The low resistivity cover is largely associated with the Quaternary volcanics and sediments and underlying Cretaceous Pirgua deposits, whereas the resistive basement is likely made by Ordovician units that crop out to the NW (Fig. 1). The thickening of the cover occurs in deep and narrow troughs where the basement is downthrown by up to 500 m. The Tocomar field shows several vertical very low resistivity "plumes" (<5 Ωm), which "cut" the basement and "spread" into the cover, where resistivity values are slightly higher (<10 Ωm).

The main faults inferred from VES, both at Tocomar and Cerro Tuzgle are oriented WNW–ESE and NE–SW.

4. Lineament detection and analysis

Remote sensing represented a useful tool for of data acquisition in the present study considering the remoteness of the area. The studied area covers 3000 km^2 but no detailed topography is available. We have used the publicly available digital elevation models (DEMs), that are from the SRTM (Shuttle Radar Topography Mission) with spatial resolution of 90 m, and from ASTER stereo-images, with

Fig. 7. (a) Example of lineaments manually traced on the "hillshade" with a light source at N 45° and 20° of inclination, and (b) on the "aspect" map of the same hillshade; (c) example of identification procedure of lineaments on the aspect map of a hillshade of a cone produced with a N 225° (±22.5°) illumination direction; the shadowed classes are blanked to enhance lineament identification; (d) lineaments identified in the study area for the same illumination as in the example in (c); (e) detail of the area shown in the box in (d); (f) traced lineaments. Note that the 1 pixel length, 2 km-equally spaced, N 340° lineaments visible in the detail area (e) are not lineaments but artefacts of the DEM.

Author's personal copy

Table 3
Number of lineaments identified for each DEM illumination condition.

Illumination direction	0°	45°	90°	135°	180°	225°	270°	315°
No. of lineaments	836	876	744	363	818	738	706	528

spatial resolution of 27.8 m. These spatial resolutions allow the performance of a lineament analysis in this mountain area with more than 2000 m of elevation contrast.

The target is the identification of the main morphostructural and structural lineament patterns that characterise the area in order to infer the role of fracturing, to define secondary permeability at the scale of the geothermal system and to generalise the data acquired during the field survey.

Some lineaments were clearly identified as faults and other known structural features that were directly observed in the field; on the other hand, most of the identified lineaments cannot be easily detected in the field (Wise et al., 1985) and are often neglected. These morphological lineaments relate to the alignment of valleys, borders of valleys, ridges, passes or, preferably, combinations of these features (Wise et al., 1985) and cluster as groups with similar azimuths and well defined regions. These groups are defined as lineament domains and are proved to be related to the recent stress conditions in the upper crust (Wise et al., 1985), thus providing useful information for describing the general fracturing and faulting pattern, as well as for better understanding the geothermal fluid circulation in the studied area.

4.1. Analysis of morphological and structural lineaments

Analysis for semi-automatically detected lineaments concentrated on a 50×60 km^2 area (Fig. 7) using the ASTER DEM from which different renderings have been created, according to 8 different, low-angle lighting conditions (shadowed images). The azimuth of most lineaments is strongly influenced by the lighting conditions: the shadow of a relief is projected on the opposite side of the valley thus producing an angle between the slope/crest alignments and their shadows and inducing an apparent rotation of these features

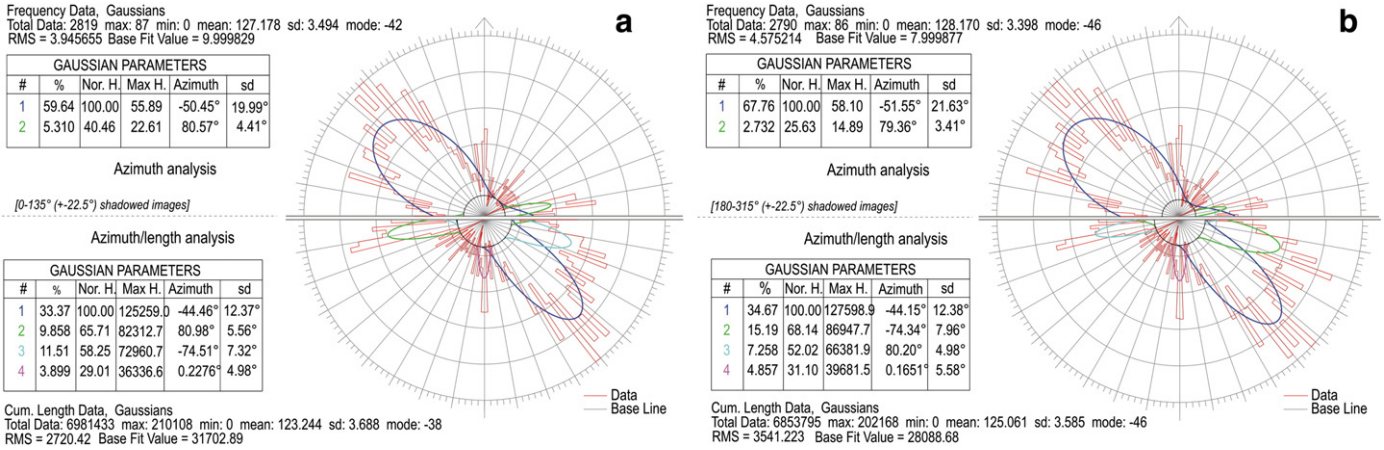

Fig. 9. Rose diagrams of lineaments' azimuthal frequency (top half) and azimuthal frequency of cumulative lineament lengths (bottom half) prepared to detect possible bias in lineament detection by the operator: (a) lineament frequency for 4 shadowed images lit from the eastern quadrant (illumination source at 0°, 45°, 90°, and 135°); (b) lineament frequency for the 4 shadowed images lit from the western quadrant (illumination source at 180°, 225°, 280°, and 315°).

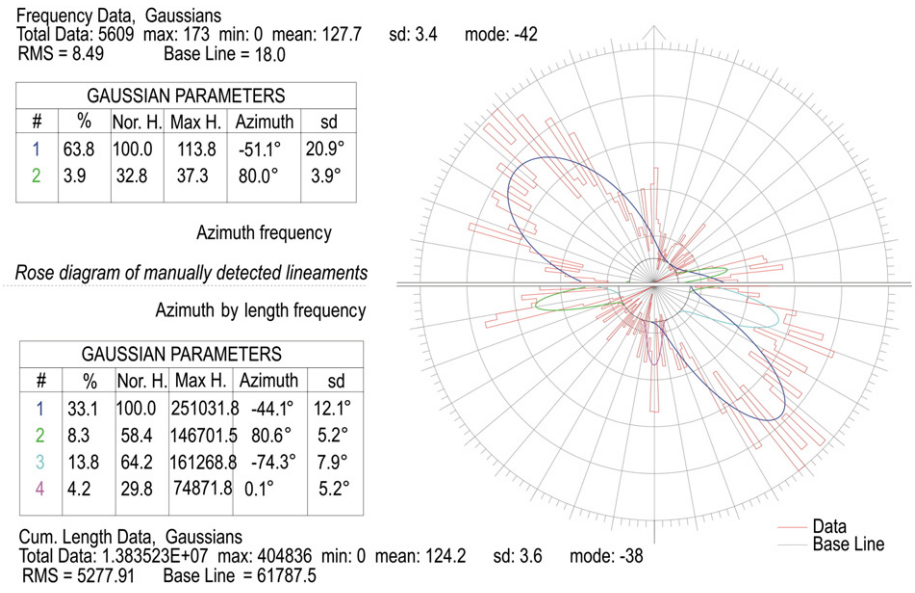

Fig. 10. Rose diagrams of manually detected lineaments directions in the upper hemisphere and the same lineaments with frequency weighted according to their length in the bottom hemisphere: longer lineaments strike NW–SE in correspondence of peak 1 and so on.

Author's personal copy

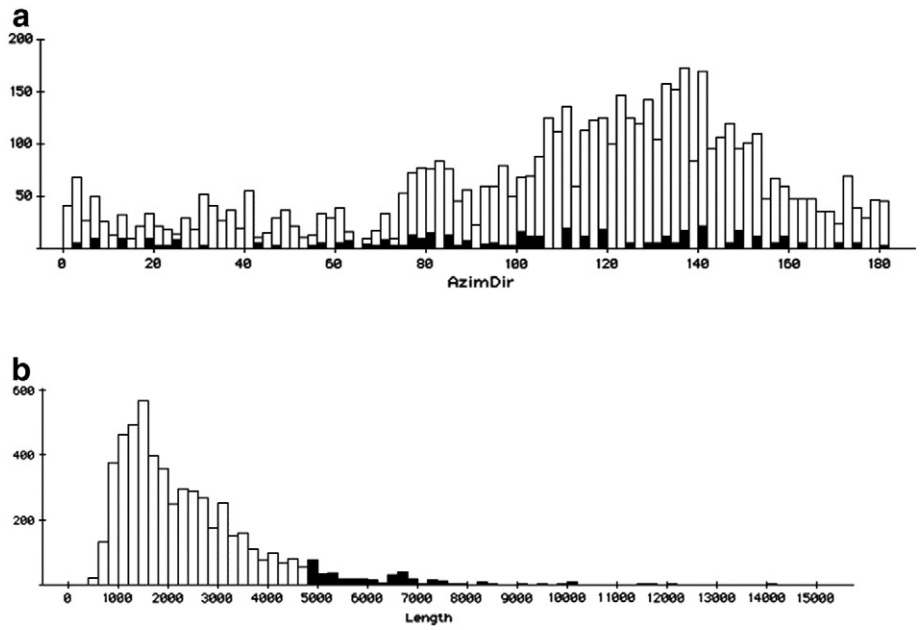

Fig. 11. (a) Lineament direction frequency histogram. (b) Lineament length frequency histogram: in black, the concentration of lineaments longer than 5 km is highlighted.

(Wise, 1969). For this reason, lineament analysis has been performed on 8 shadowed images (hillshades) with different lighting directions (0°, 45°, 90°, 135°, 180°, 235°, 270° and 315°).

Each shadowed image has been filtered by the aspect function (software ArcGIS™), thus allowing the identification of directions of the maximum slope (0–360°). The aspect directions have been subdivided into 8 classes: $0° \pm 22.5°$, $45° \pm 22.5°$, ..., $315° \pm 22.5°$ and were colour coded. The same class direction with their associated colour code was used for each filtered image. Flat areas and classes facing the opposite sense of the lighting direction, together with the two adjacent classes, were blanked in each filtered image (Fig. 7). This procedure eases the visual detection and tracing of lineaments following the same colours, which correspond to slopes and morphologies similarly oriented.

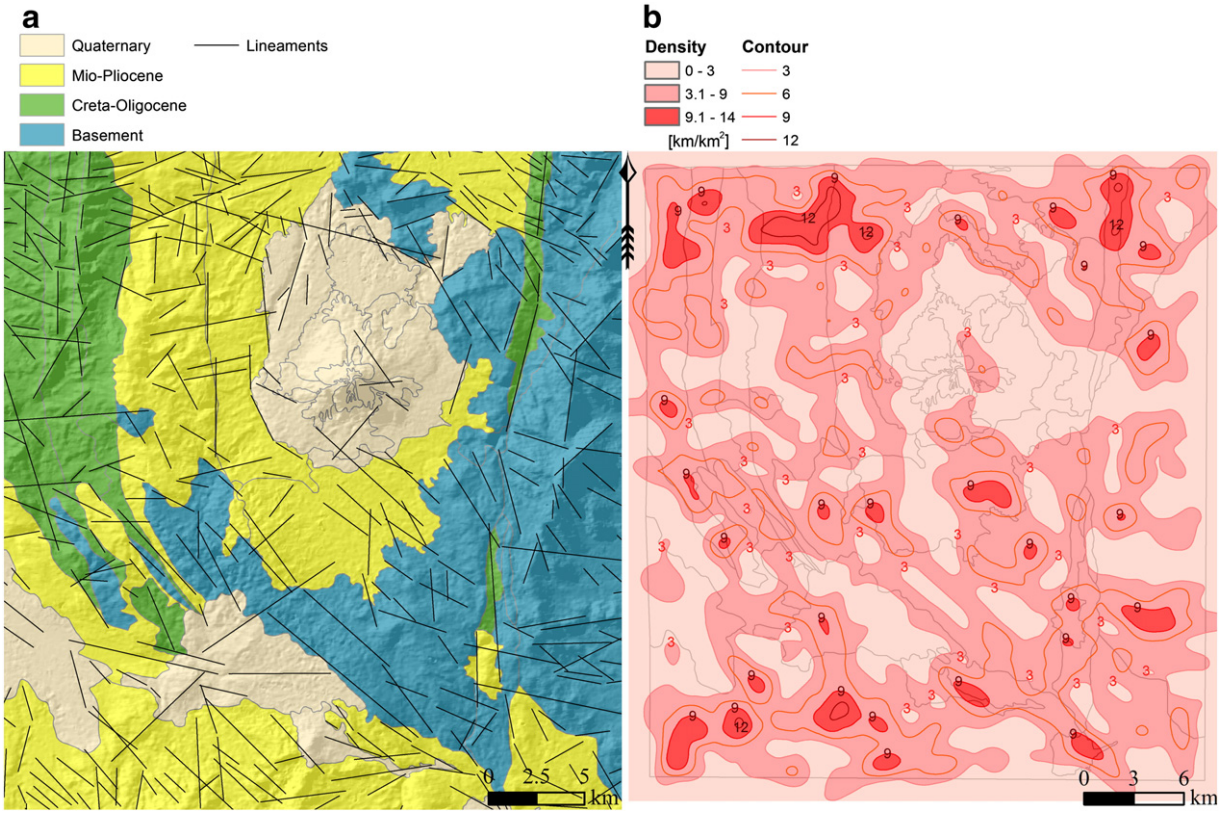

Fig. 12. (a) Semi-automatically detected lineaments overlapped on the simplified geology of the area (see text). (b) Lineament density map (km of lineaments for km^2).

Author's personal copy

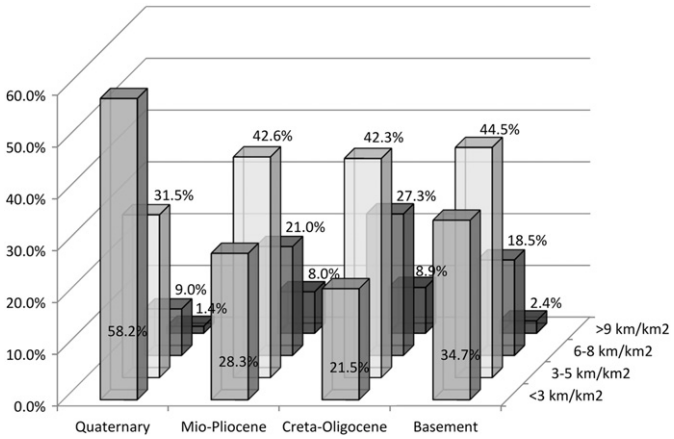

Fig. 13. Percentage of lineament density classes per rock-groups.

The local scale lineament analysis allowed the detection of a total of 5609 lineaments of variable length from 442 m to 14,070 m and an average length of 2466 m (Fig. 8). The number of lineaments detected for each lighting condition is presented in Table 3.

Since lineaments observed in more than one lighting condition are better defined (Figs. 9–14), we have maintained the total number of detected lineaments (i.e. the sum of all lineaments also where overlapping) as a weighing factor for statistical analysis.

Since the knowledge of the geology of the area may bias the judgement of the operator when visually identifying and manually drawing the lineaments, it is essential to verify the actual objectivity of the lineament identification results. Identified lineaments have been therefore divided into two groups according to the lighting conditions (lighting directions for group 1: 0°, 45°, 90°, 135°; lighting directions for group 2: 180°, 235°, 270° and 315°). The azimuthal frequency of the two groups was statistically analysed and results were plotted in rose diagrams (Fig. 9). The similarity of the two groups testifies for the reliability of the lineament identification technique.

The most frequent azimuthal orientation by number and by cumulated length is NW–SE ± 20° (Fig. 10). Subordinate orientations are ENE–WSW ± 15° and N–S ± 10°. The frequency of lineament directions weighted by cumulated lengths shows that the WNW–ESE direction is also important and bears relatively longer lineaments (Fig. 10).

The frequency length distribution is positively skewed (Fig. 11a) and the most frequent lineament length is 1.4 km. Lineaments longer than 5 km are present in most of the azimuthal directions, but are proportionally more relevant for the N–S, ENE–WSW and WNW–ESE directions, with respect to the main NW–SE group (Fig. 11b).

Further analyses have been carried out for highlighting possible relationships between lineaments and outcropping rock-formations. Stratigraphic units have been grouped as: Paleozoic basement, Cretaceous–Oligocene formations, Miocene–Pliocene formations and Quaternary formations (Fig. 12a). Density of lineaments on Quaternary formations is generally lower than 3 km/km^2, whereas on older rocks it generally

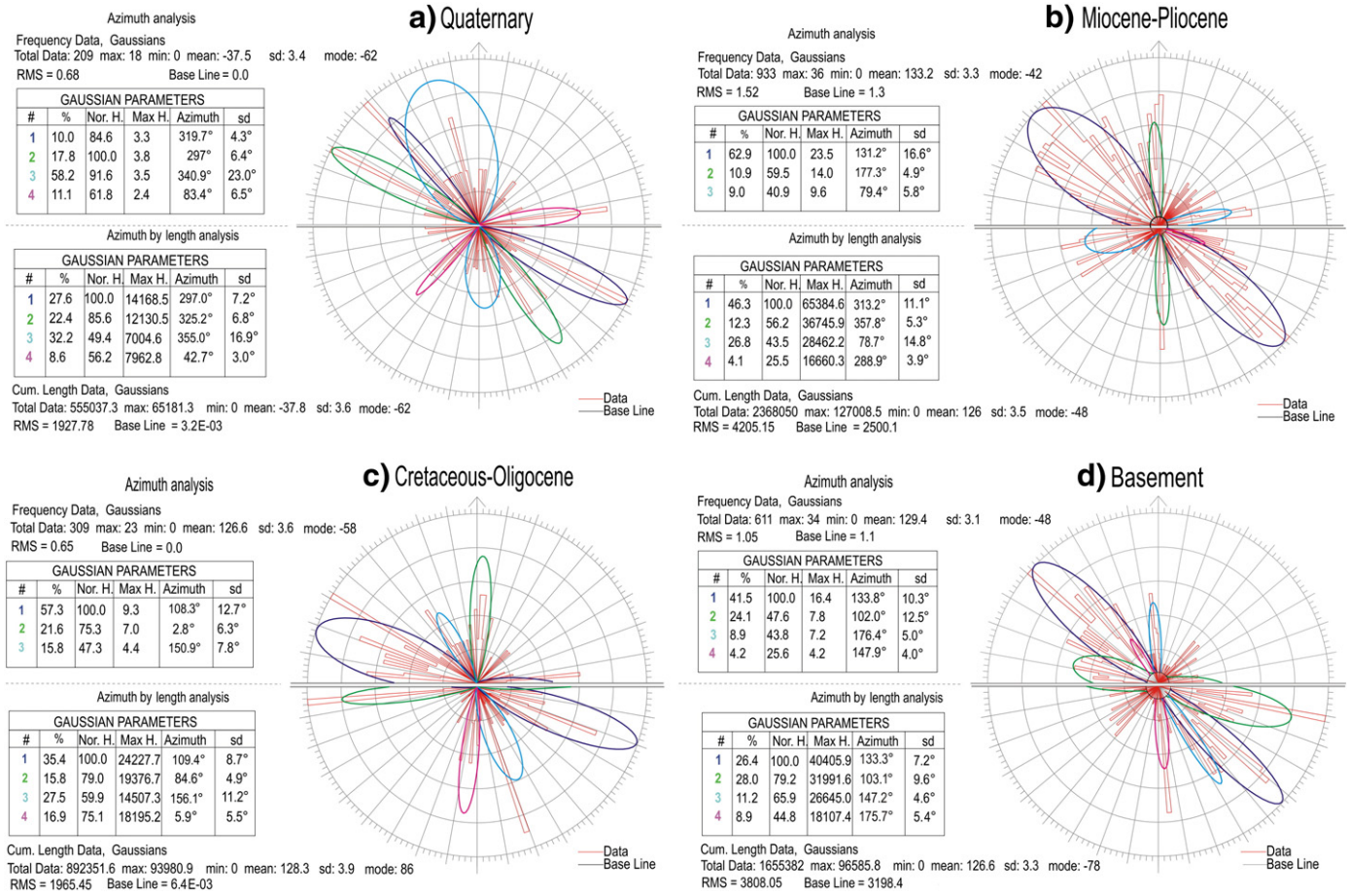

Fig. 14. Azimuthal frequency rose diagram (top half) and azimuthal frequency cumulated with length (bottom half) for the (a) Quaternary units, (b) Miocene–Pliocene units, (c) Cretaceous–Oligocene units and (d) basement units.

Author's personal copy

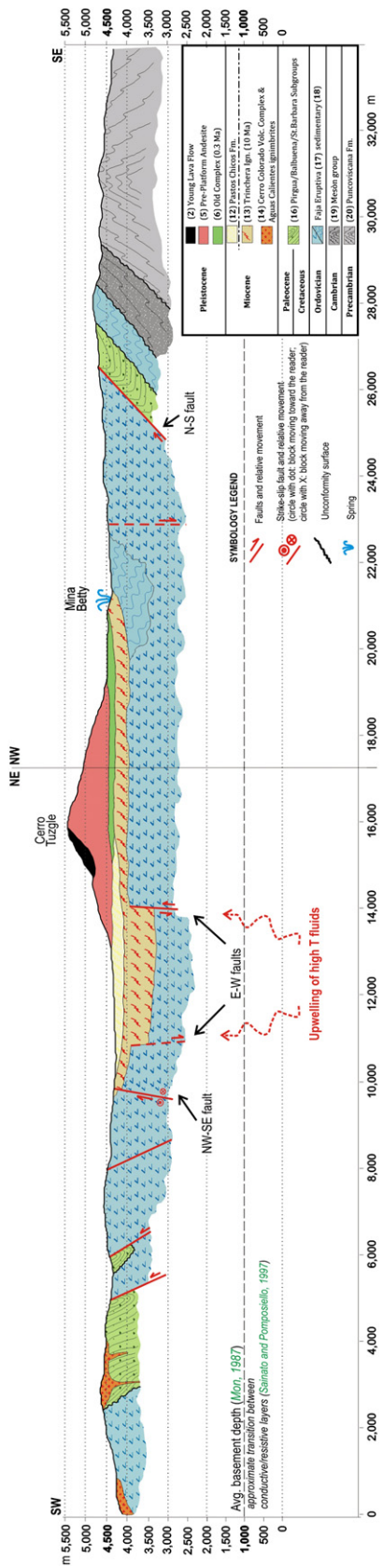

Fig. 15. Schematic cross section across the Cerro Tuzgle geothermal field.

Author's personal copy

exceeds this value, reaching 9 to 12 km/km^2, particularly in the northwestern area and in the Tocomar-COT zone (Fig. 1). In Fig. 13 the histogram shows the frequency (%) of lineaments for each class of density, compared with rock ages: in the Quaternary rocks the percentage of areas with low density of lineaments (<3 km/km^2) is higher with respect to areas with higher densities and also with respect to older rocks. For Miocene–Pliocene, Cretaceous–Oligocene and Paleozoic basement rocks, on the contrary, lineaments with densities between 3 and 8 km/km^2 are dominant, whereas densities higher than 9 km/km^2 characterise more the Miocene–Pliocene and Cretaceous–Oligocene groups. The rose diagrams of Fig. 14 show frequency analysis by number and by cumulated length of lineaments for each of the 4 rock-groups. Quaternary rocks (Fig. 14a) are intersected by variously oriented lineaments, mainly around the NW–SE and E–W directions, with the NW–SE lineaments by far the longest. The Miocene–Pliocene rocks are intersected dominantly by NW–SE lineaments, which are also the longest, with secondary N–S and ENE–WSW (Fig. 14b). Cretaceous–Oligocene rocks are dominated by WNW–ESE lineaments that are also the longest, with secondary orientations directed N–S and NNW–SSE (Fig. 14c). NW–SE lineaments are also dominant on the Paleozoic basement, together with the WNW–ESE direction that has longer lineaments (Fig. 14d).

5. Discussion

The revision of the stratigraphic, structural and hydrogeological framework of the Cerro Tuzgle–Tocomar area and the re-interpretation of geoelectric data indicate that geothermal circulation is controlled by the presence of regional and local fracture systems which allow localised geothermal fluids upwelling through the Ordovician basement (Fig. 15). We identify the fractured Paleozoic basement units, characterised by unevenly distributed secondary permeability, as the geothermal reservoir, which may coincide with that proposed from magnetotelluric data by Sainato and Pomposiello (1997) with its top between 0.8 and 2 km depth.

Recharge areas are the high altitude ridges above 4500 m a.s.l that bound the Tuzgle depression (Figs. 1 and 4); these areas are largely made of fractured Ordovician basement rocks (to the east and to the south) and by the Miocene Cerro Colorado dacite intrusions (to the west).

At lower elevations (<4500 m a.s.l.), the poorly permeable and discontinuous Tertiary–Quaternary cover that fills the wide Tuzgle depression and the Tocomar basin seals locally the fractured basement, though hosting a poorly to locally moderately productive phreatic groundwater circulation (Fig. 15), where geothermal fluids can spread and drift in the form of plumes (Fig. 6). The thermal springs of the area, i.e. Tocomar, Aguas Calientes, Pompeya, and Mina Betty, occur where the cover or the basement are cut through by incised valleys in correspondence to the localised, fracture-controlled upwelling of geothermal fluids (Fig. 4).

Since permeability in the reservoir is due to fracturing, the reconstruction of the fracture fabric is essential to understand the preferential circulation of the geothermal fluids and to define the appropriate methodology to quantify the geothermal potential of the area (Muffler and Cataldi, 1978).

The lineament analysis (Figs. 7–14) shows that the longer and most frequent lineaments are directed NW–SE, ENE–WSW and N–S (Fig. 10). These directions correspond to the strike of the main regional tectonic structures (see Petrinovic et al., 2006; Acocella et al., 2011) that are: the N–S ridges related to the compressional Tertiary Andean orogenetic phases; the NW–SE left-lateral COT fault system and associated secondary structures such as the extensional ENE–WSW faults and fractures that dominate where the main segments of the COT are over-stepping, such as in the Tocomar area (Fig. 1; e.g. Petrinovic et al., 2006). The structural significance of lineaments is confirmed by the analysis of the lineament density (Fig. 12), which shows how areas of higher densities of lineaments (>9 km/km^2) are aligned along the main tectonic structures. In particular NW–SE lineaments parallel to the COT and associated ENE–WSW extensional structures cut all units (Fig. 14), including the Quaternary rocks, maintaining the predominance over the other secondary orientations that are characterised by shorter lineaments. The presence of NW–SE lineaments parallel to the COT distributed over the entire study area suggests that associated fractures can also be found not only in correspondence of the COT, as in the Tocomar geothermal field, but also well away from the main fault system, as for the Cerro Tuzgle geothermal field; moreover, permeability can be considerably increased by the concurrent intersection with minor fractures. As a matter of fact, the Tocomar field is the most productive, both in terms of water discharge and of temperature of the geothermal water at springs. The springs of the Tuzgle field are instead less productive and at lower temperatures, suggesting that the intersection of the main COT and the secondary extensional structures at Tocomar indeed produce a much more permeable system (cf. Petrinovic et al., 2006).

Given the presence of active tectonic structures in the study area (Petrinovic et al., 2006; Acocella et al., 2011), it can be argued that a spatial variation of permeability exists and that this would cause hydraulic gradients to focus the flux of waters (Cox et al., 2001) along structures that allow migration towards the surface, as observed in the geoelectric profiles (Fig. 6). In the study area, left-lateral, strike-slip and en-echelon COT segments form a wide releasing band (or an incipient pull-apart basin) in the Tocomar area: a favourable structural framework for increasing vertical permeability and for fluid upwelling, both magmatic and hydrothermal, justifying the presence of volcanic centres and of geothermal systems. The presence of the newly discovered maars or phreatic craters in the Tocomar area can be explained by taking into account that extensional movements can lead to an abrupt decrease in fluid pressure, causing hydraulic brecciation and phreatic explosions (Sibson, 2001; Cas et al., 2011).

In order to have fluid upwelling along the detected structures, it is essential that deep reservoirs are indeed present and that these reservoirs are intercepted by those structures. According to geophysical data (Sainato and Pomposiello, 1997) the reservoir top is at 0.8–2 km depth, and the bottom is between 3.1 and 3.6 km. According to Cox et al. (2001), in the first kilometre of the upper crust, fracturing and permeability are high and fluid pore pressure is generally equivalent to the hydrostatic pressure, while at deeper levels, the loss of pore connectivity leads to an increase in fluid pressure reaching the lithostatic pressure, so that it is likely for a deep reservoir to have a suprahydrostatic pressure (provided that a non permeable level seals the reservoir). Thus, it is possible that the active and permeable fault system and its suite of fractures and shear zones, have intercepted the deeper part of the reservoir, causing a fast migration of fluids towards the surface, driven by the pressure gradient. Active faulting and fracturing of the basement rocks allow depressurization of fluids kept in the deep part of the reservoir, enabling a prompt leakage (e.g. Tocomar field) and mixing between hot deep fluids and shallow cold waters, as indicated by available geochemical data (Coira, 1995).

Our model suggests that any future study aimed at the development of the geothermal fields in the Cerro Tuzgle–Tocomar volcanic area should carefully define the local fracture patterns and that remote sensing and field-based structural analyses are essential to identify the best suited areas for location of productive deep-drillings.

6. Conclusions

Our model for the Cerro Tuzgle–Tocomar geothermal field locates the main reservoir within the Pre-Palaeozoic–Ordovician basement units, permeable for intense fracturing. The reservoir is locally covered by the low permeable Miocene–Quaternary units that allow poor circulation of groundwater, wherein geothermal fluids upwelled along the fractured basement spread and drift. Main recharge areas are identified in the high altitude ridges, >4500 m a.s.l. They are mainly

Author's personal copy

characterised by fractured Ordovician units that we identify as the main shallow reservoir.

The detection of lineaments from digital elevation models shows that the main orientations correspond to the directions of the main regional tectonic structures: the N–S compressional ridges relative to the Andean orogenetic phases and the NW–SE left-lateral COT fault system (distributed over the entire study area), with associated ENE–WSW secondary structures. The density of lineaments is higher (>9 km/km^2) along these orientations. The main NW–SE and ENE–WSW directions cut all units. The intersection of principal and secondary structures allow an increased permeability that justifies the higher productivity of the Tocomar geothermal field (in terms of water discharge and temperature), while the Cerro Tuzgle field hosts lesser productive springs as this concurrent intersection of structures is less developed. Furthermore, in this latter case, the presence of a shallow aquifer in the Tuzgle depression causes a mixing between hot deep and cold shallow fluids that explain the geochemical signature of these springs.

Supplementary data to this article can be found online at http://dx.doi.org/10.1016/j.jvolgeores.2012.09.009.

Acknowledgments

This work was supported by a CNR-Curiosity Driven 2008 grant (Tettonica attiva, risalita di fluidi geotermici e pericolosità ambientale lungo il sistema tettonico di trasferimento Calama–Olacapato–Toro, Ande centrali — Argentina; Resp. Gianluca Groppelli) and the CONICET grant PIP 127 (Resp. Jose Viramonte). We are very grateful to Dr. Giorgio Stangalino (AREA GEOFISICA ENG. S.A. — Buenos Aires, Argentina) for allowing the use and interpretation of unpublished vertical electrical soundings. We thank F. Salvini for discussion and guidance on lineament analysis. We also acknowledge Don Wise and an anonymous reviewer for constructive comments that helped in improving the final version of this paper.

References

Aceñolaza, F., Aceñolaza, G., 2005. La formación Puncoviscana y unidades estratigráficas vinculadas en el neoproterozoico — cámbrico temprano del noroeste argentino. Latin American Journal of Sedimentology and Basin Analysis 12 (2), 65–87.

Acocella, V., Gioncada, A., Omarini, R., Riller, U., Mazzuoli, R., Vezzoli, L., 2011. Tectonomagmatic characteristics of the back-arc portion of the Calama–Olacapato–El Toro Fault Zone, Central Andes. Tectonics 30, TC3005 (19 pp.).

Aguilera, Felipe A., 2008. Origen y naturaleza de los fluidos en los sistemas volcánicos, geotermales y termales de baja entalpía de la Zona Volcánica Central (ZVC) entre los 17° 43 ′S y 25° 10′ S. PhD Thesis. Antofagasta, Chile

Allmendinger, R.W., Ramos, V.A., Jordan, T.E., Palma, M., Isacks, B.L., 1983. Paleogeography and Andean structural geometry, northwest Argentina. Tectonics 2 (1), 1–16.

Allmendinger, R.W., Jordan, T.E., Kay, S.M., Isacks, B.L., 1997. The evolution of the Altiplano-Puna Plateau of the Central Andes. Annual Review of Earth and Planetary Sciences 25, 139–174.

Aquater, 1980. Exploración geotérmica del áarea del Cerro Tuzgle, Provincia de Jujuy, Argentina. Secretaría de Estado de Minería. Unpublished report.

Barberi, F., Innocenti, F., Landi, P., Rossi, U., Saitta, M., Santacroce, R., Villa, I.M., 1984. The evolution of Latera caldera (central Italy) in the light of subsurface data. Bulletin of Volcanology 47 (1), 125–141.

Bear, A.N., Giordano, G., Giampaolo, C., Cas, R.A.F., 2009. Volcanological constraints on the post-emplacement zeolitisation of ignimbrites and geoarchaeological implications for Etruscan tomb construction (6th–3rd century B.C.) in the Tufo Rosso a Scorie Nere, Vico Caldera, Central Italy. Journal of Volcanology and Geothermal Research 183 (3–4), 183–200.

Bibby, H.M., Caldwell, T.G., Davey, F.J., Webb, T.H., 1995. Geophysical evidence on the structure of the Taupo Volcanic Zone and its hydrothermal circulation. Journal of Volcanology and Geothermal Research 68, 29–58.

Blasco, G., Zappettini, E., Hongn, F., 1996. Hoja Geológica 2566-I, San Antonio de los Cobres, provincias de Salta y Jujuy, 1:250,000. Buenos Aires, Boletín, 217. Servicio Geológico Minero de Argentina.

Brogi, A., 2003. Extensional shear zones as imaged by reflection seismic lines: the Larderello geothermal field (central Italy). Tectonophysics 363, 127–139.

Cas, R., Giordano, G., Balsamo, F., Esposito, A., Lo Mastro, S., 2011. Hydrothermal breccia textures and processes: Lisca Bianca islet, Panarea volcano, Aeolian islands, Italy. Society of Economic Geologists Inc. Economic Geology 106, 437–450.

Coira, B., 1973. Resultados preliminares sobre la petrología del ciclo eruptivo Ordovícico concomitante con la sedimentación de la Formación Acoite en la zona de Abra Pampa, prov. de Jujuy. Revista de la Asociación Geológica Argentina 28, 85–88.

Coira, B., 1995. Cerro Tuzgle geothermal prospect, Jujuy, Argentina. Proceedings of the World Geothermal Congress, 2, Florence, Italy, pp. 1161–1165.

Coira, B., Kay, S.M., 1993. Implications of Quaternary volcanism at Cerro Tuzgle for crustal and mantle evolution of the Puna Plateau, Central Andes, Argentina. Contributions to Mineralogy and Petrology 113, 40–58.

Cox, S.F., Knackstedt, M.A., Braun, J., 2001. Principles of structural control on permeability and fluid flow in hydrothermal systems. Society of Economics Geologists Reviews 14, 1–24.

CREGEN Centro Regional de Energíia Geotérmica del Neuquén, 1988. Estudio geotérmico del área Tuzgle-Tocomar-Pompeya. Unpublished.

DeSilva, S.L., Gosnod, W.D., 2007. Episodic construction of batholiths: insight from the spatiotemporal development of an ignimbrite flare-up. Journal of Volcanology and Geothermal Research 167, 320–335.

Ferretti, J., 1998. Caracterización de las Fuentes termales asociadas a los complejos volcánicos Quevar-Cerro Verde-Aguas Calientes. Relevamiento e interpretación de datos gravimétricos y geoeléctricos. Informe Final, FOMEC-Universidad Nacional de Salta, (inédito), Salta . (123 pp.).

Ferretti, J., Alonso, R., 1993. Geoquímica del campo geotérmico Tocomar (Salta). XII Congreso Geológico Argentino. II Congreso de Exploración de Hidrocarburos. Buenos Aires, Argentina.

Fournier, R.O., Truesdell, A.H., 1973. An empirical Na–K–Ca geothermometer of natural water. Geochimica et Cosmochimica 37, 1255–1275.

Fournier, R.O., White, D.E., Truesdell, A.H., 1974. Geochemical indicators of subsurface temperature. Part I, basic assumptions. Journal Research U.S. Geological Survey 2 (3), 259–262.

Garcia-Castellanos, D., 2006. Long-term evolution of tectonic lakes: climatic controls on the development of internally drained basins. In: Willett, S.D., Hovius, N., Brandon, M.T., Fisher, D.M. (Eds.), Tectonics, Climate and Landscape Evolution. Geological Society of America Special Paper 398, Penrose Conference Series, pp. 283–294 http://dx.doi.org/10.1130/2006.2398(17).

Geotermia Andina, S.A., 2008. Geothermal energy in Argentina. Internal Report. Calle Humberto Primo No. 985 Piso 5-Of. 3 C.A.P. 1103, Buenos Aires. Argentina.

Giggenbach, W.F., Gonfiantini, R., Jangi, B.L., Truesdell, A.H., 1983. Isotopic and chemical composition of Partoati Valey geothermal discharges, NW Himalaya, India. Geothermics 12, 199–222.

Hidroproyectos, S.A., Stec, S.R.L., Sepic, S.C., 1984. Estudio de la segunda fase de prefactibilidad geotérmica del área denominada Tuzgle. Departamento de Susques, Provincia de Jujuy. Ministerio de Economía, dirección de Minería, Jujuy.

Hilton, D., Hammerschmidt, K., Teufel, S., Friedrichsen, H., 1993. Helium isotope characteristics of Andean geothermal fluids and lavas. Earth and Planetary Science Letters 120, 265–282.

Matteini, M., Mazzuoli, R., Omarini, R., Cas, R., Maas, R., 2002a. The geochemical variations of the upper Cenozoic volcanism along the Calama–Olacapato–El Toro transversal fault system in central Andes (24° S): petrogenetic and geodynamic implications. Tectonophysics 345, 211–227.

Matteini, M., Mazzuoli, R., Omarini, R., Cas, R., Maas, R., 2002b. Geodynamical evolution of the central Andes at 24° S as inferred by magma composition along the Calama–Olacapato–El Toro transversal volcanic belt. Journal of Volcanology and Geothermal Research 118, 205–228.

Mazzuoli, R., Vezzoli, L., Omarini, R., Acocella, V., Gioncada, A., Matteini, M., Dini, A., Guillou, H., Hauser, N., Uttini, A., Scaillet, S., 2008. Miocene magmatism and tectonics of the easternmost sector of the Calama–Olacapato–El Toro fault system in Central Andes at 24° S: insights into the evolution of the Eastern Cordillera. Geological Society of America Bulletin 120 (11–12), 1493–1517.

Mendez, V., Navarini, N., Plaza, D., Viera, O., 1973. Faja Eruptiva de la Puna Oriental. V Congreso geológico Argentino Actas 4, 89–100.

Moreno, J.A., 1970. Estratigrafia y Paleogeografía del Cretácico Superior de la Cuenca del Noroeste Argentino, con especial mensión a del Subgrupos Balbuena y Santa Bárbara. Revista de la Asociación geológica Argentina 24, 9–44.

Moreno Espelta, M.C., Viramonte, J.G., Arias, J.E., 1975. Geología del área termal de Rosario de la Frontera y sus posibilidades geotécnicas. Actas del segundo congreso Ibero-Americano de Geología Económica IV, pp. 543–548.

Muffler, P., Cataldi, R., 1978. Methods for regional assessment of geothermal resources. Geothermics 7, 53–89.

Muffler, L.J.P., Duffield, W.A., 1995. The role of volcanic geology in the exploration for geothermal energy. Proceedings of the World Geothermal Congress, 2, Florence, Italy, pp. 657–662.

Pesce, A., 1999. Geotermia. 14° Congreso Geológico Argentino. Relatorio 2, 69–98.

Pesce, A.E., 2010. Argentina country update. Proceedings World Geothermal Congress 2010 Bali, Indonesia, April 25–29.

Petrinovic, I.A., Mitjavila, J., Viramonte, J.G., Marti, J., Becchio, R., Arnosio, M., 1999. Geoquímica y geocronologia de secuencias volcánicas neogenas de trasarco en el extremo oriental de la Cadena Volcanica Transversal del Quevar, NO de Argentina. Acta Geológica Hispánica 34, 255–272.

Petrinovic, I.A., Arnosio, J.M., Alvarado, G.E., Guzmán, S., 2005. Erupciones freáticas sintectónicas en el campo geotérmico de Tocomar, Salta. Revista de la Asociación Geológica Argentina 60 (1), 132–141.

Petrinovic, I.A., Riller, U., Brod, E.R., Alvarado, G.E., Arnosio, J.M., 2006. Bimodal volcanism in a tectonic transfer zones: evidence for tectonically controlled magmatism in the southern central Andes, NW Argentina. Journal of Volcanology and Geothermal Research 152, 240–252.

Petrinovic, I.A., Martí, J., Aguirre Díaz, G.J., Guzmán, S., Geyer, A., Salado Paz, N., 2010. The Cerro Águas Calientes caldera, NW Argentina: an example of a tectonically

Author's personal copy

controlled, polygenetic collapse caldera, and its regional significance. Journal of Volcanology and Geothermal Research 194, 15–26.
Reutter, K.J., 2001. Le ande centrali: elementi di un'orogenesi di margine continentale attivo. Acta Naturalia de "L'ateneo Parmense" 37 (1/2), 5–37.
Reyes, F.C., Salfity, J.A., 1973. Cosideraciones sobre la estratigrafia del Cretácico (Subgrupo Pirgua) del Noeste Argentino. Congreso Geologico Argentino Actas 3, 355–385.
Ricci, M., Figueroa, L.A., 1971. Fotolienamientos y mineralizaciones en Noroeste Argentino. Dirección nacional de Geología y Minería, San Miguel de Tucumán, Argentina.
Riller, U., Petrinovic, I.A., Ramelow, J., Greskowiak, J., Strecker, M., Onken, O., 2001. Late Cenozoic tectonism, caldera and plateau formation in the central Andes. Earth and Planetary Science Letters 188, 299–311.
Sainato, C.M., Pomposiello, M.C., 1997. Two-dimensional magnetotelluric and gravity models of the Tuzgle volcano zone (Jujuy Province, Argentina). Journal of South American Earth Sciences 10, 247–261.
Salfity, J.A., 1985. Lineamientos transversales al rumbo andino en el Noroeste Argentino. 4° Congreso Geológico Chileno. Actas (1–2), 119–137.
Salfity, J.A., Monaldi, C.R., 2006. Hoja Geológica 2566-IV: Metán (1:250,000). Programa Nacional de Cartas Geológicas de la República Argentina, boletin N. 319, Buenos Aires. (80 pp.).
Schurr, B., Asch, G., Rietbrock, A., Kind, R., Pardo, M., Heit, B., Monfret, T., 1999. Seismicity and average velocities beneath the Argentine Puna plateau. Geophysical Research Letters 26, 3025–3028.
Schwab, K., 1973. Die Stratigraphie in der Umgebung des Salar de Cauchari (NW-Argentinien). Ein Beitrag zur erdgeschichtlichen Entwicklung der Puna (Stratigraphy of the Salar de Cauchari region (NW-Argentina)). Geotectonic Research 43 (ISBN 978-3-510-50009-3).
Schwab, K., Lippolt, H., 1976. K–Ar mineral ages and late Cenozoic history of the Salar Cauchari area (Argentina, Puna). In: Gonzales-Ferran, O. (Ed.), Proceedings of the Symposium on Andean and Antarctic Volcanological Problems: Santiago, International Association of the Volcanology and Chemistry of the Earth's Interior Special Series, pp. 698–714.
Seggiaro, R., Aguilera, N., Gallardo, E., Ferretti, J., 1997. Structure and geothermic potential of the Rosario de la Frontera thermal area, Salta, Argentina. VIII Congreso Geològico Chileno Actas 1 (2), 390–394.
Sibson, R.H., 2001. Seismogenic framework for hydrothermal transport and ore deposition. Society of Economics Geologists Reviews 14, 25–50.
Sierra, J.L., Pedro, G., 1988. Estudio geotérmico del área Tuzgle–Tocomar–Pompeya. Centro Regional de Energía Geotérmica del Neuquén (CREGEN). Neuquén (informe inédito).
Sobel, E.R., Hilley, G.E., Strecker, M.R., 2003. Formation of internally drained contractional basins by aridity-limited bedrock incision. Journal of Geophysical Research 108 (B7), 2344.
Tonda, R., Kirschbaum, A., Pettinari, G., Arnosio, M., 2010. Stratigraphy and Mineralogy of the First Abandoned Mine Tailing of the Concordia Mine, Salta, Argentina. 18th IAS International Sedimentological Congress, 2010 Mendoza, Argentina.
Turner, J.C.M., 1964. Descripción de la Hoja Geológica 7c, Nevado de Cachi. Boletín, 99. Dirección Nacional de Geología y Minería, Salta.
Viramonte, J.G., Galliski, M.A., Araña Saavedra, V., Aparicio, A., Garcia Cacho, L.Y., Martín Escorza, C., 1984. El finivolcanismo básico de la depresión de Arizaro, provincia de Salta. IX Congreso Geológico Argentino Actas I, pp. 234–251.
Viramonte, J.M., Becchio, R., Viramonte, J., Pimentel, M., Martino, R., 2007. Ordovician igneous and metamorphic units in the southern Puna: new U/Pb and Sm/Nd data and implications for the evolution of NW Argentina. Journal of South American Earth Sciences 24 (2–4), 167–183.
Wise, D.U., 1969. Regional and sub-continental sized fracture systems detectable by topographic shadow techniques. Geological Society of Canada Paper 68–52, 175–199.
Wise, D.U., Funiciello, R., Parotto, M., Salvini, F., 1985. Topographic lineament swarms: clues to their origin from domain analysis of Italy. Geological Society of America Bulletin 96, 952–967.
Wood, C.P., 1995. Calderas and geothermal systems in the Taupo Volcanic zone, New Zealand. Proceedings of the World Geothermal Congress, Florence, Italy, pp. 1331–1336.
Wright, H.W., Lesti, C., Cas, R.A.F., Porreca, M., Viramonte, J., Folkes, C.B., Giordano, G., 2011. Columnar jointing in vapor phase altered Cerro Galan ignimbrite, Paycuqui, Argentina. In: Cashman, K., Cas, R.A.F. (Eds.), The Geology of the Cerro Galan Caldera System, Northwestern Argentina. Spec. Issue Bulletin of Volcanology. http://dx.doi.org/10.1007/s00445-011-0524-6.